

The Differential Assembly of the Centers and Outskirts of Main Sequence Galaxies at $z \sim 2.3$

Sam Cutler

2nd Year Talk

Advisor: Mauro Giavalisco

A brief overview

Introduction

Background

Existing theories of
galaxy structural
component formation

Sample selection

Analysis

Bulge detection and
decompositions

SED fitting: *Prospector*

Dealing with unresolved
photometry

Results

Detections

Star formation histories
and bulge formation

Future tests and analyses

Introduction

Background

Existing theories of
galaxy structural
component formation

Sample selection

Analysis

Bulge detection and
decompositions

SED fitting: *Prospector*

Dealing with unresolved
photometry

Results

Detections

Star formation histories
and bulge formation

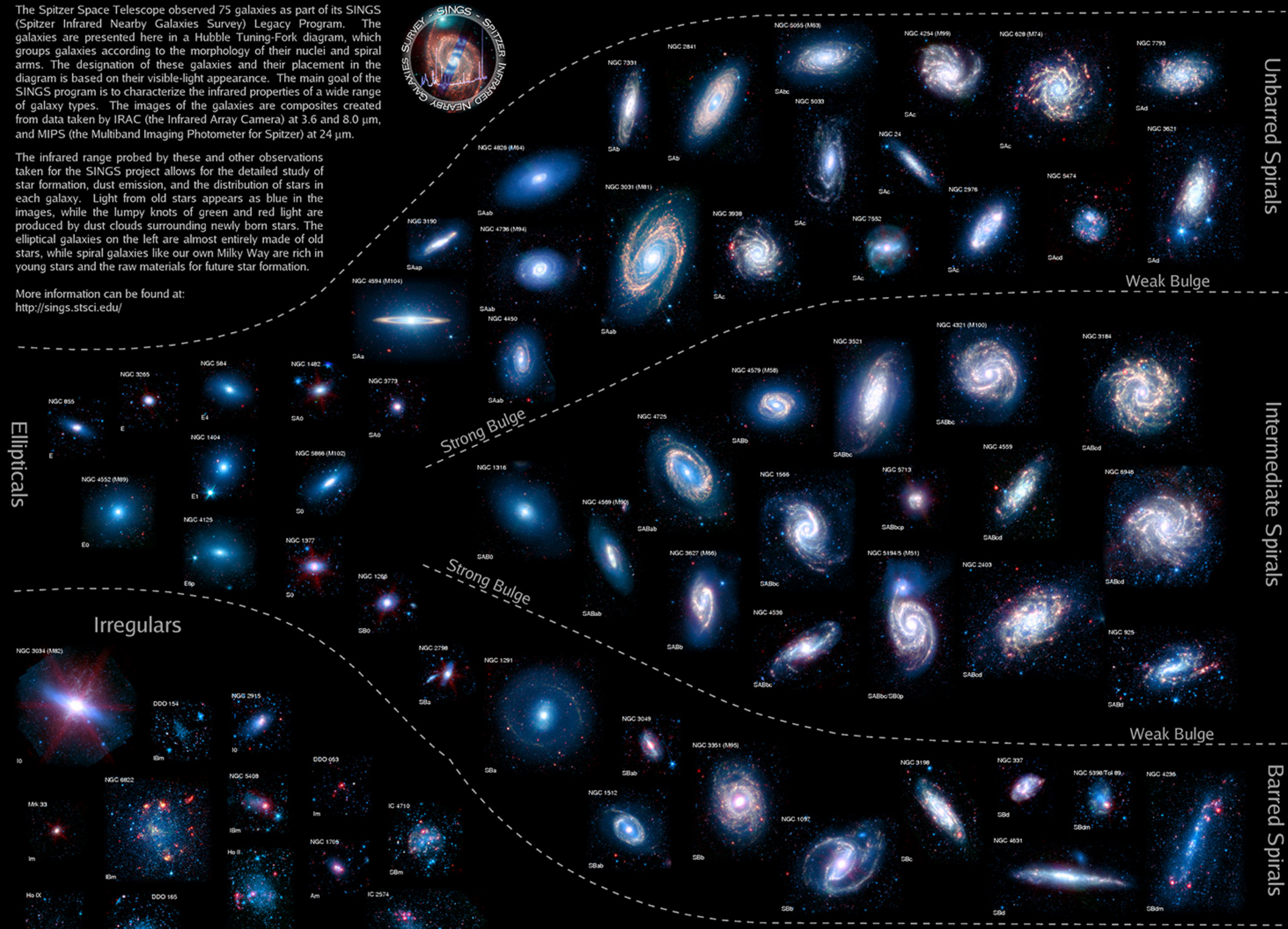
Future tests and analyses

The Spitzer Infrared Nearby Galaxies Survey (SINGS) Hubble Tuning-Fork

The Spitzer Space Telescope observed 75 galaxies as part of its SINGS (Spitzer Infrared Nearby Galaxies Survey) Legacy Program. The galaxies are presented here in a Hubble Tuning-Fork diagram, which groups galaxies according to the morphology of their nuclei and spiral arms. The designation of these galaxies and their placement in the diagram is based on their visible-light appearance. The main goal of the SINGS program is to characterize the infrared properties of a wide range of galaxy types. The images of the galaxies are composites created from data taken by IRAC (the Infrared Array Camera) at 3.6 and 8.0 μm , and MIPS (the Multiband Imaging Photometer for Spitzer) at 24 μm .

The infrared range probed by these and other observations taken for the SINGS project allows for the detailed study of star formation, dust emission, and the distribution of stars in each galaxy. Light from old stars appears as blue in the images, while the lumpy knots of green and red light are produced by dust clouds surrounding newly born stars. The elliptical galaxies on the left are almost entirely made of old stars, while spiral galaxies like our own Milky Way are rich in young stars and the raw materials for future star formation.

More information can be found at: <http://sings.stsci.edu/>



Ellipticals

Irregulars

Strong Bulge

Strong Bulge

Weak Bulge

Weak Bulge

Unbarred Spirals

Intermediate Spirals

Barred Spirals



Poster and composite images created from SINGS observations by Karl D. Gordon (Oct 2007)
 Blue=IRAC 3.6 μm (stars)
 Green=IRAC 8 μm (aromatic features from dust grains/molecules)
 Red=MIPS 24 μm (warm dust)

SINGS Team
 Robert Kennicutt, Jr. (Principle Investigator), Daniela Calzetti (Deputy Principle Investigator), Charles Engelbracht (Technical Contact), Lee Armus, George Bendo, Caroline Bot, Brent Buckalew, John Cannon, Daniel Dale, Bruce Draine, Karl Gordon, Albert Grauer, David Hollenbach, Tom Jarrett, Lisa Kewley, Claus Leitherer, Aigen Li, Sangeeta Malhotra, Martin Meyer, John Moustakas, Eric Murphy, Michael Regan, George Rieke, Marcia Rieke, Helene Roussel, Kartik Sheth, J.D. Smith, Michele Thornley, Fabian Walter & George Helou

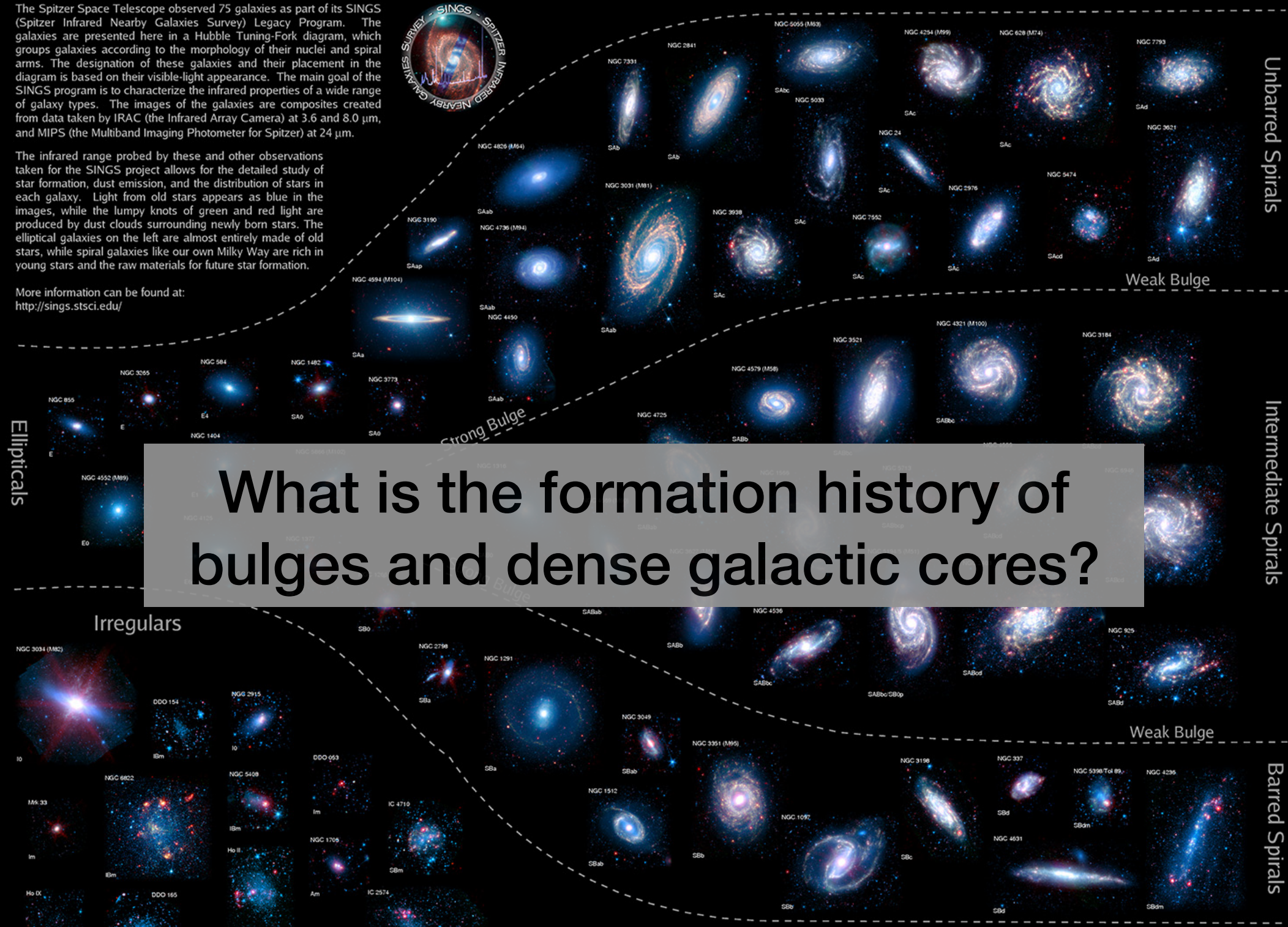
SINGS Team

The Spitzer Infrared Nearby Galaxies Survey (SINGS) Hubble Tuning-Fork

The Spitzer Space Telescope observed 75 galaxies as part of its SINGS (Spitzer Infrared Nearby Galaxies Survey) Legacy Program. The galaxies are presented here in a Hubble Tuning-Fork diagram, which groups galaxies according to the morphology of their nuclei and spiral arms. The designation of these galaxies and their placement in the diagram is based on their visible-light appearance. The main goal of the SINGS program is to characterize the infrared properties of a wide range of galaxy types. The images of the galaxies are composites created from data taken by IRAC (the Infrared Array Camera) at 3.6 and 8.0 μm , and MIPS (the Multiband Imaging Photometer for Spitzer) at 24 μm .

The infrared range probed by these and other observations taken for the SINGS project allows for the detailed study of star formation, dust emission, and the distribution of stars in each galaxy. Light from old stars appears as blue in the images, while the lumpy knots of green and red light are produced by dust clouds surrounding newly born stars. The elliptical galaxies on the left are almost entirely made of old stars, while spiral galaxies like our own Milky Way are rich in young stars and the raw materials for future star formation.

More information can be found at: <http://sings.stsci.edu/>



What is the formation history of bulges and dense galactic cores?

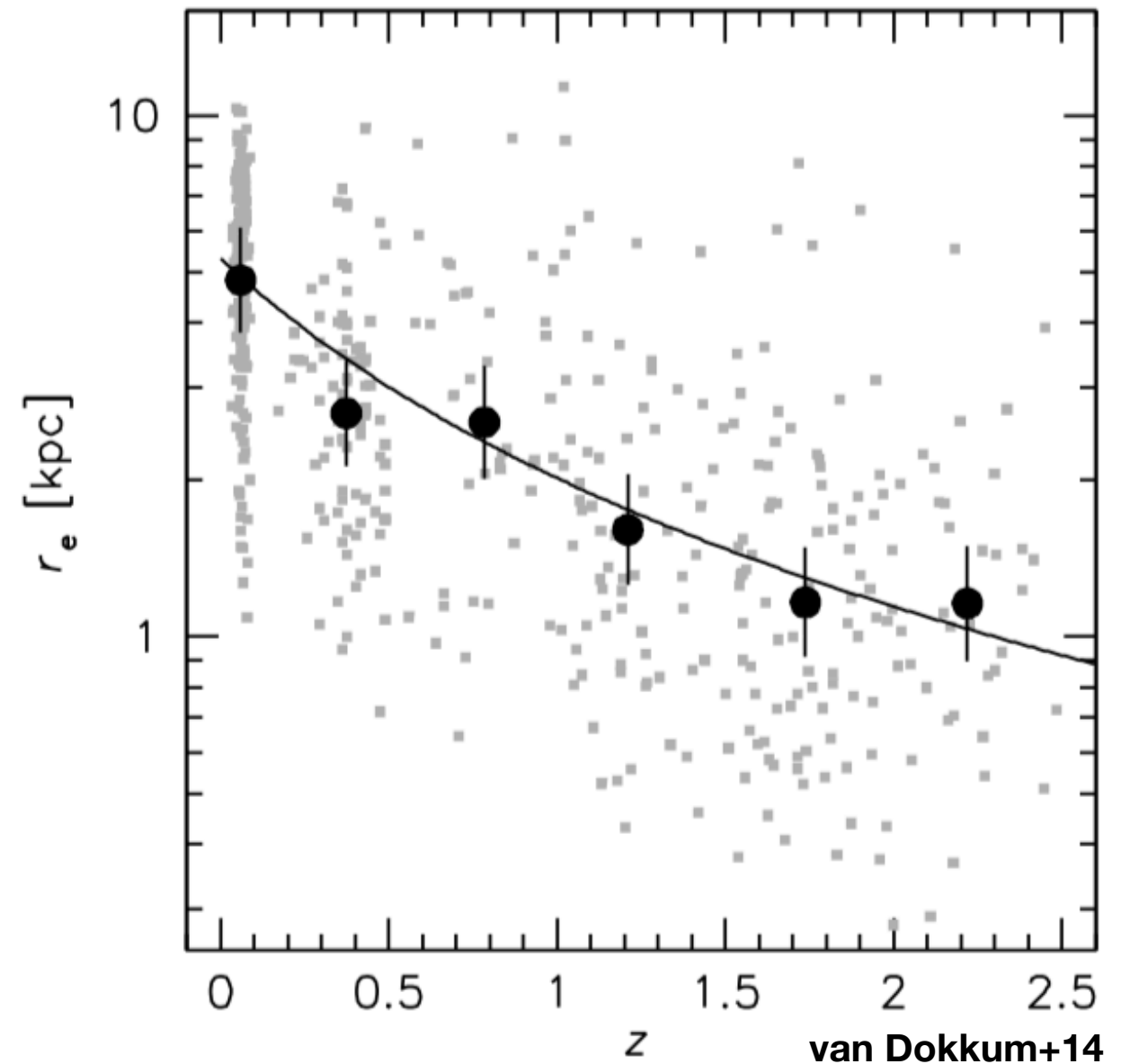
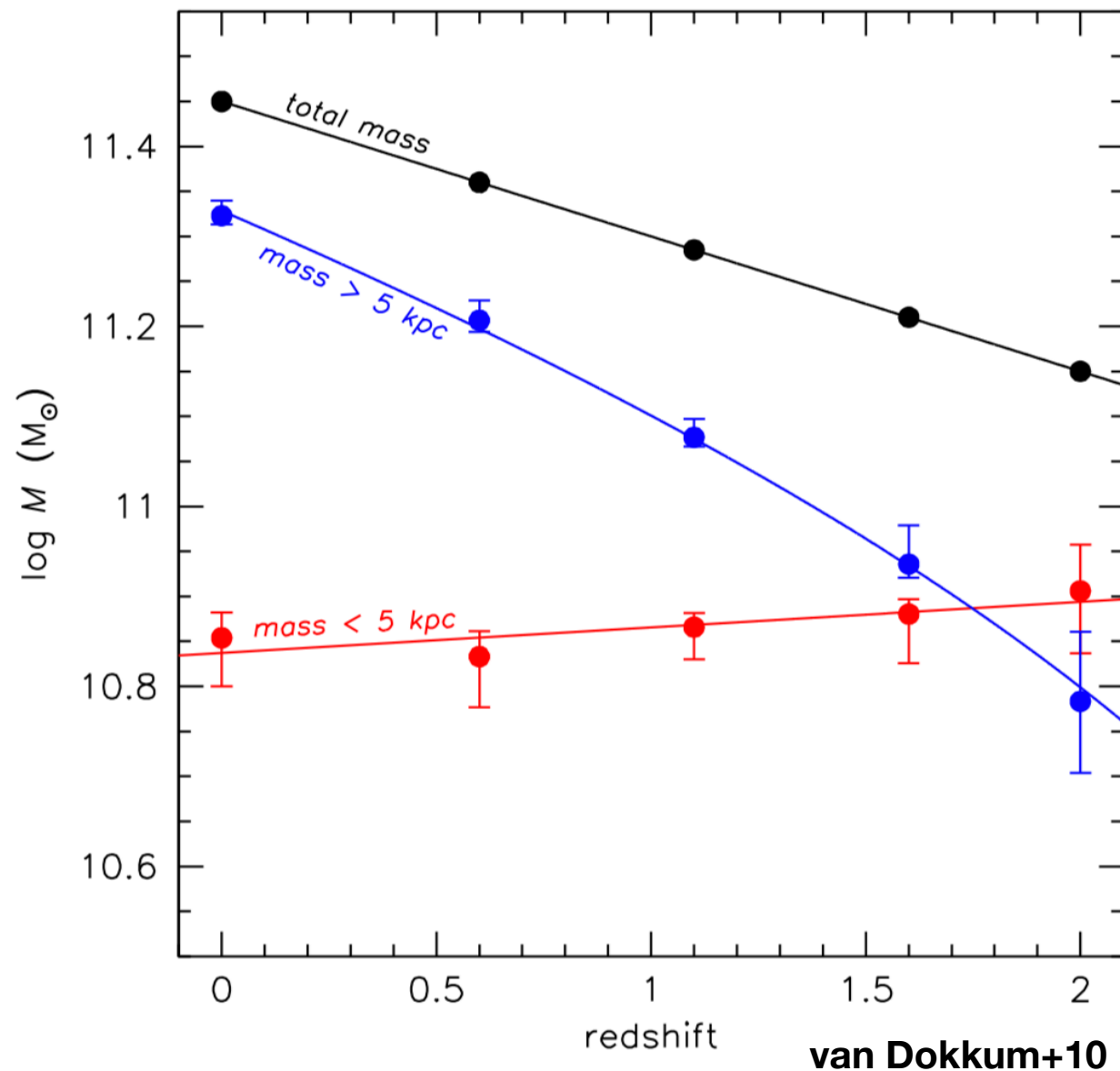


Poster and composite images created from SINGS observations by Karl D. Gordon (Oct 2007)
 Blue=IRAC 3.6 μm (stars)
 Green=IRAC 8 μm
 (aromatic features from dust grains/molecules)
 Red=MIPS 24 μm (warm dust)

SINGS Team
 Robert Kennicutt, Jr. (Principle Investigator), Daniela Calzetti (Deputy Principle Investigator), Charles Engelbracht (Technical Contact), Lee Armus, George Bendo, Caroline Bot, Brent Buckalew, John Cannon, Daniel Dale, Bruce Draine, Karl Gordon, Albert Grauer, David Hollenbach, Tom Jarrett, Lisa Kewley, Claus Leitherer, Aigen Li, Sangeeta Malhotra, Martin Meyer, John Moustakas, Eric Murphy, Michael Regan, George Rieke, Marcia Rieke, Helene Roussel, Kartik Sheth, J.D. Smith, Michele Thornley, Fabian Walter & George Helou

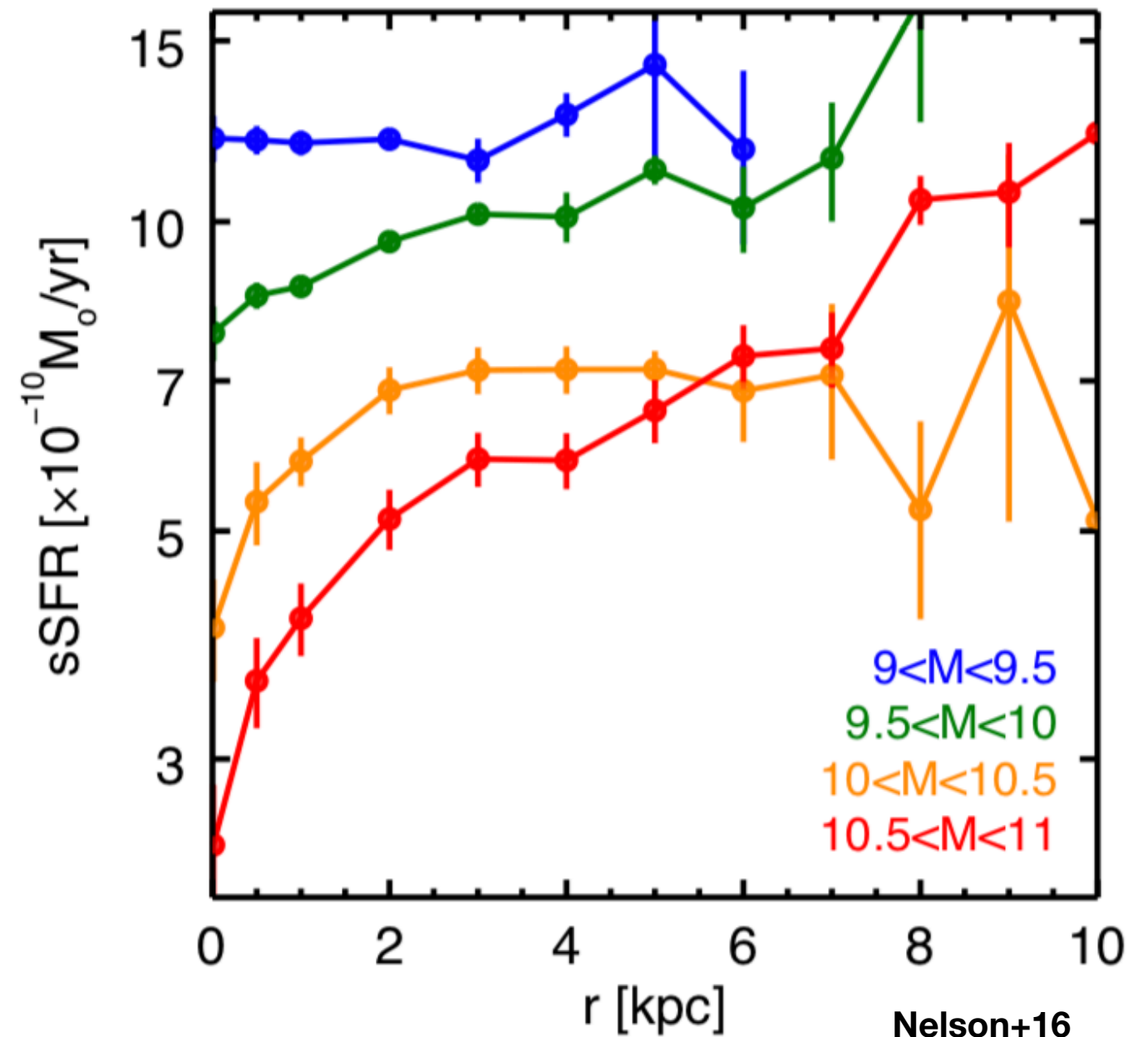
Massive galaxies

Compact central regions already in place by $z \sim 2.5$



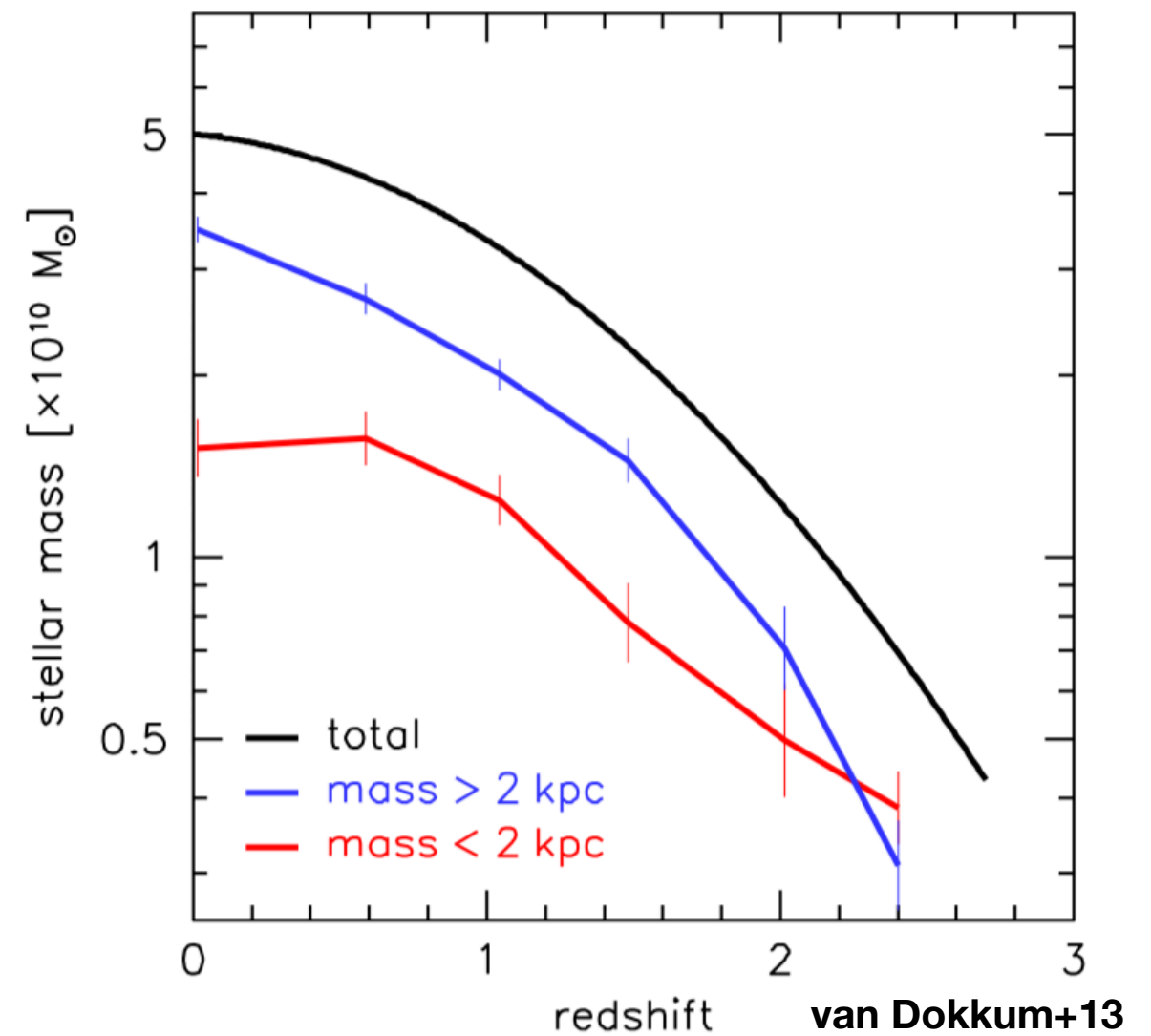
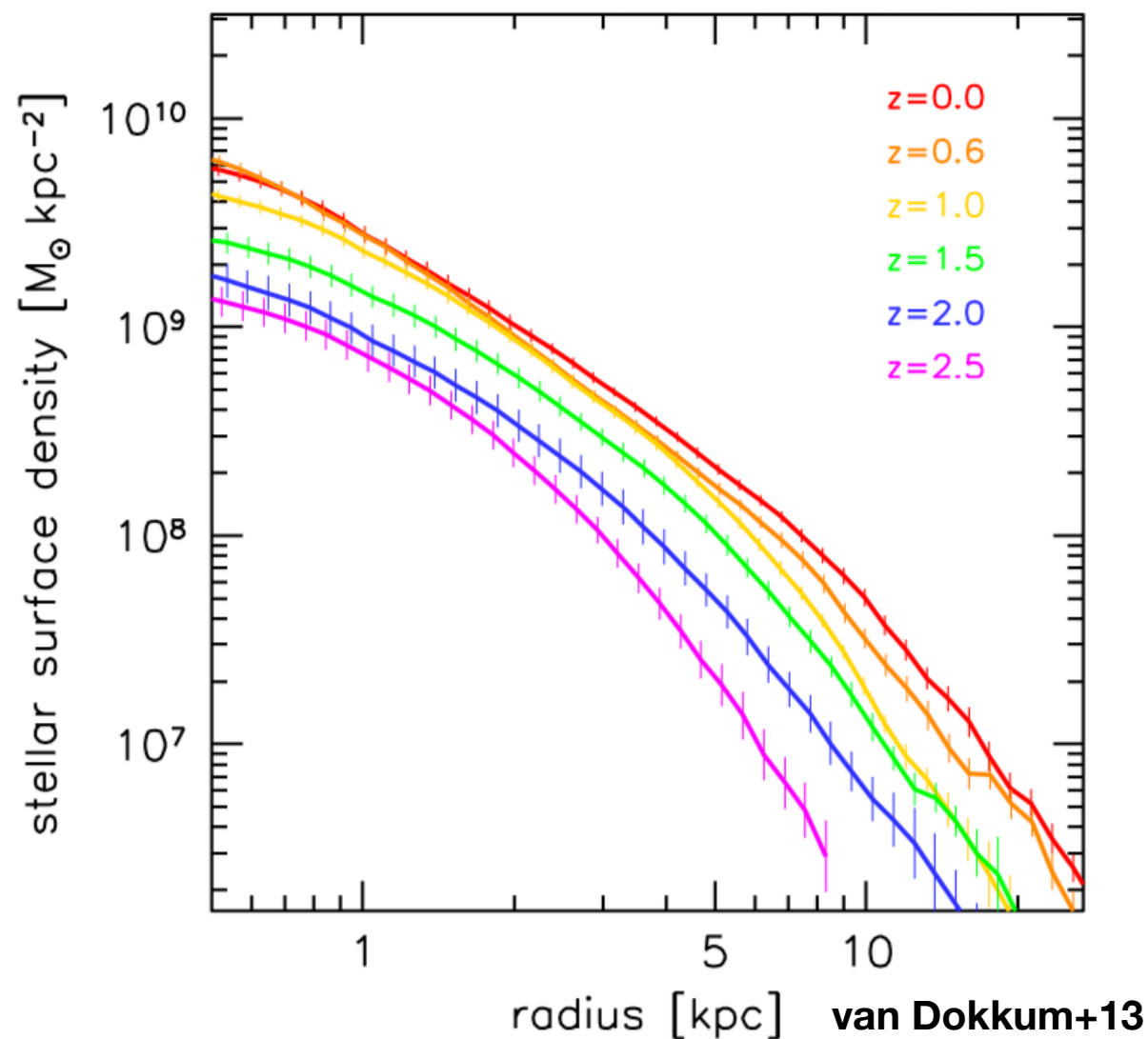
Inside-out formation?

- Massive galaxies form central parts first
- sSFR rates are elevated at large radii at $z \sim 1$
- Centers of spirals are formed at high redshift (“naked bulges”)?

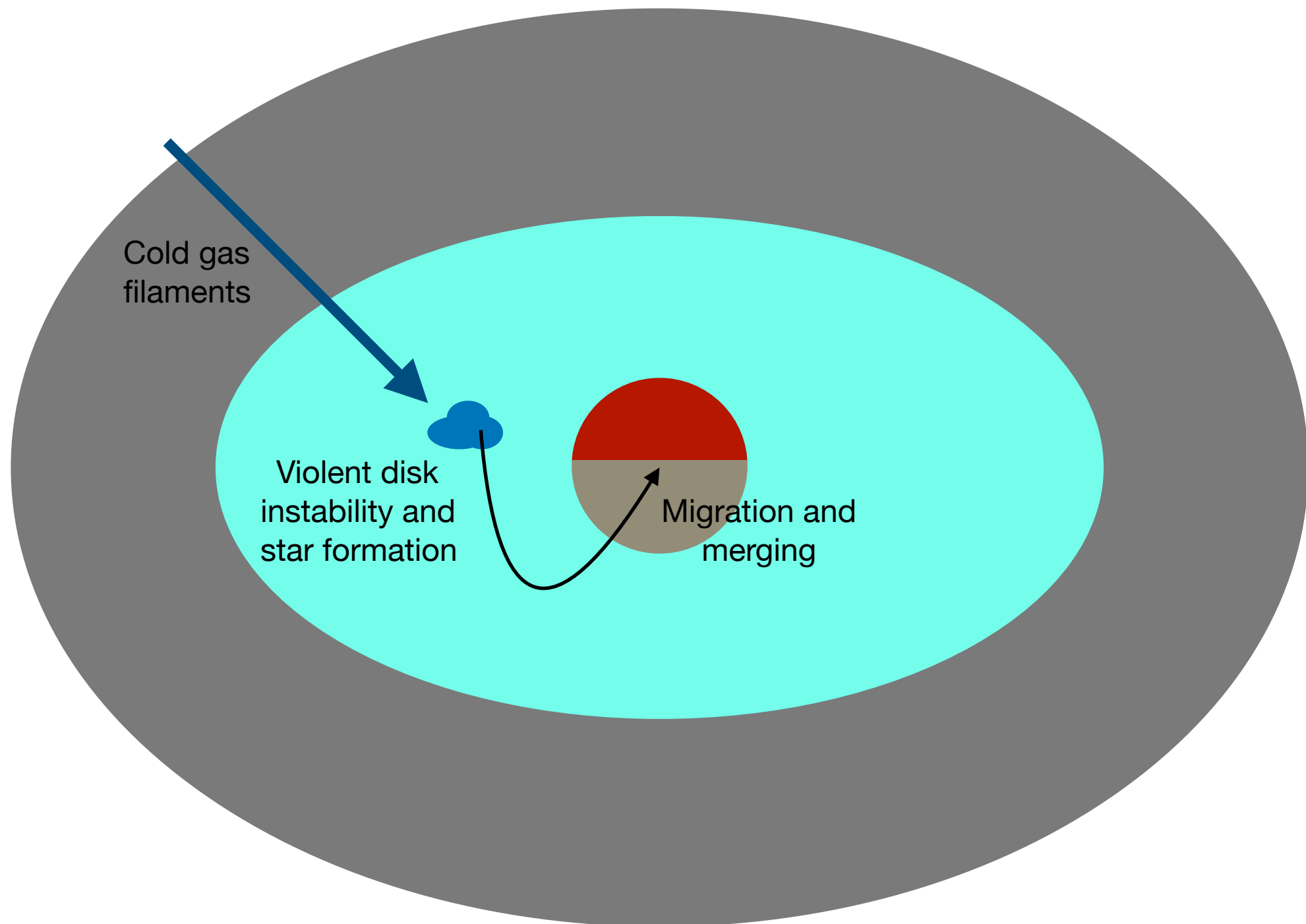


Milky-Way-like galaxies

Bulges built up at same time as disks: no naked bulges!

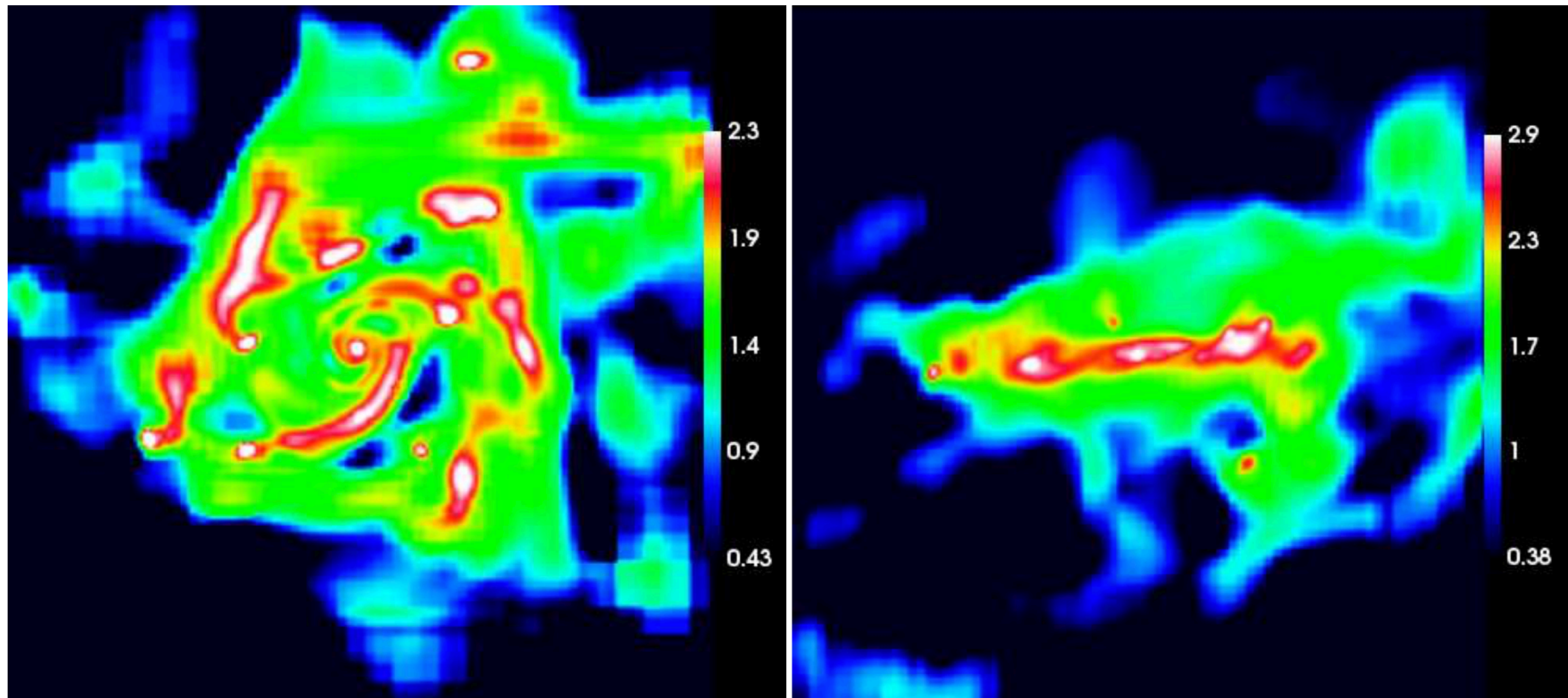


Bulge formation by gas accretion and clump migration



Bulge formation by gas accretion and clump migration

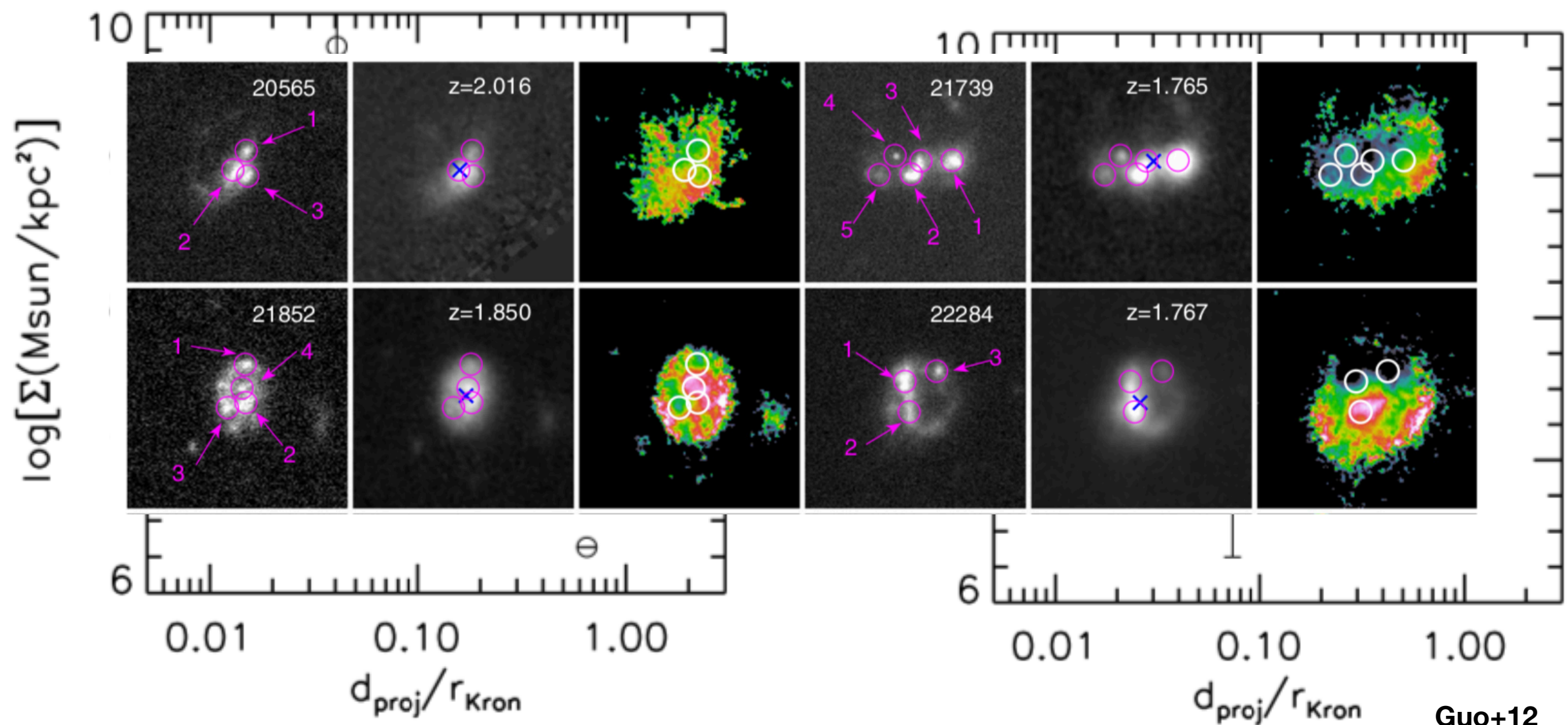
Seen in hydrodynamic simulations



Ceverino+09, Dekel+09

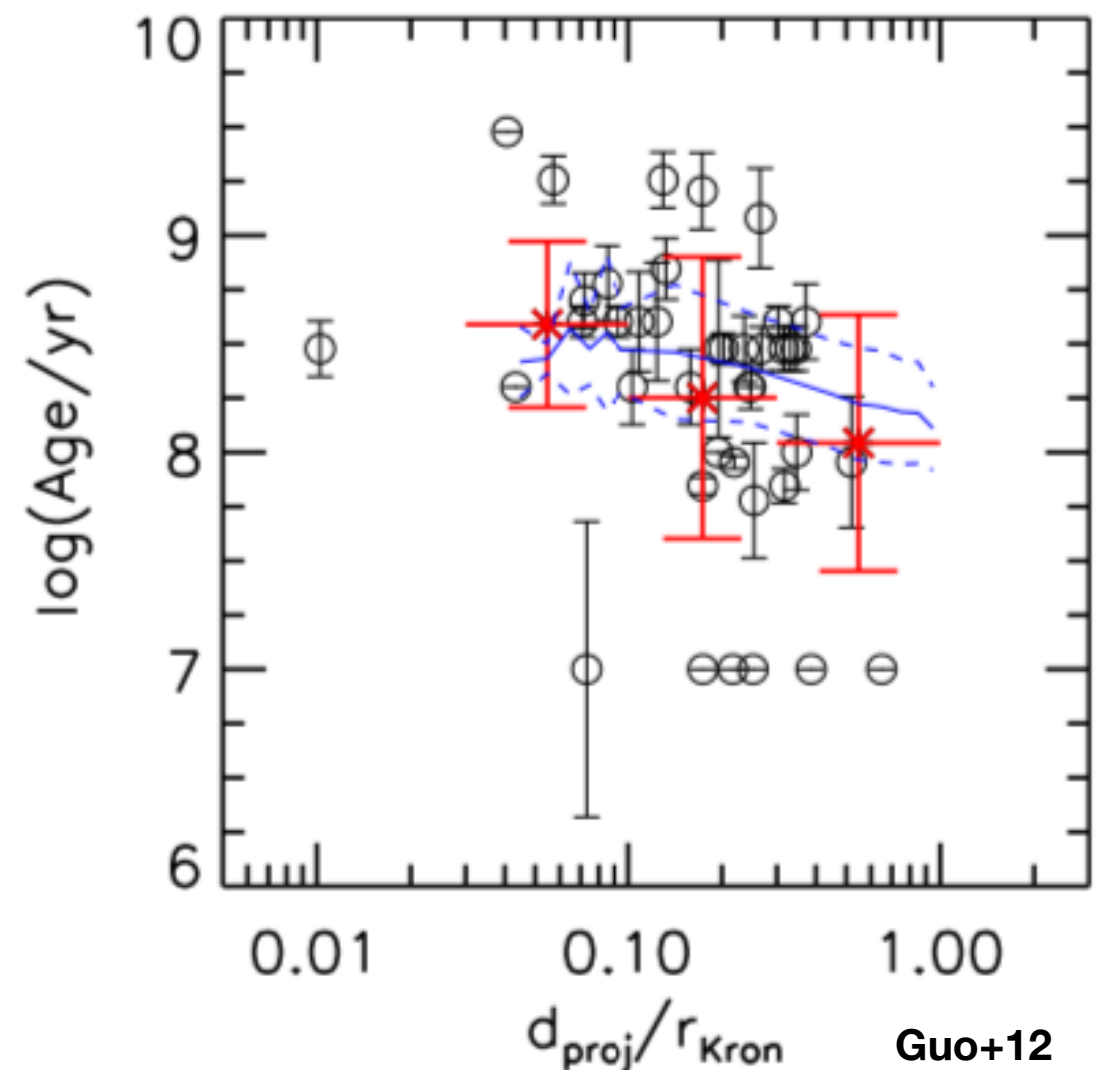
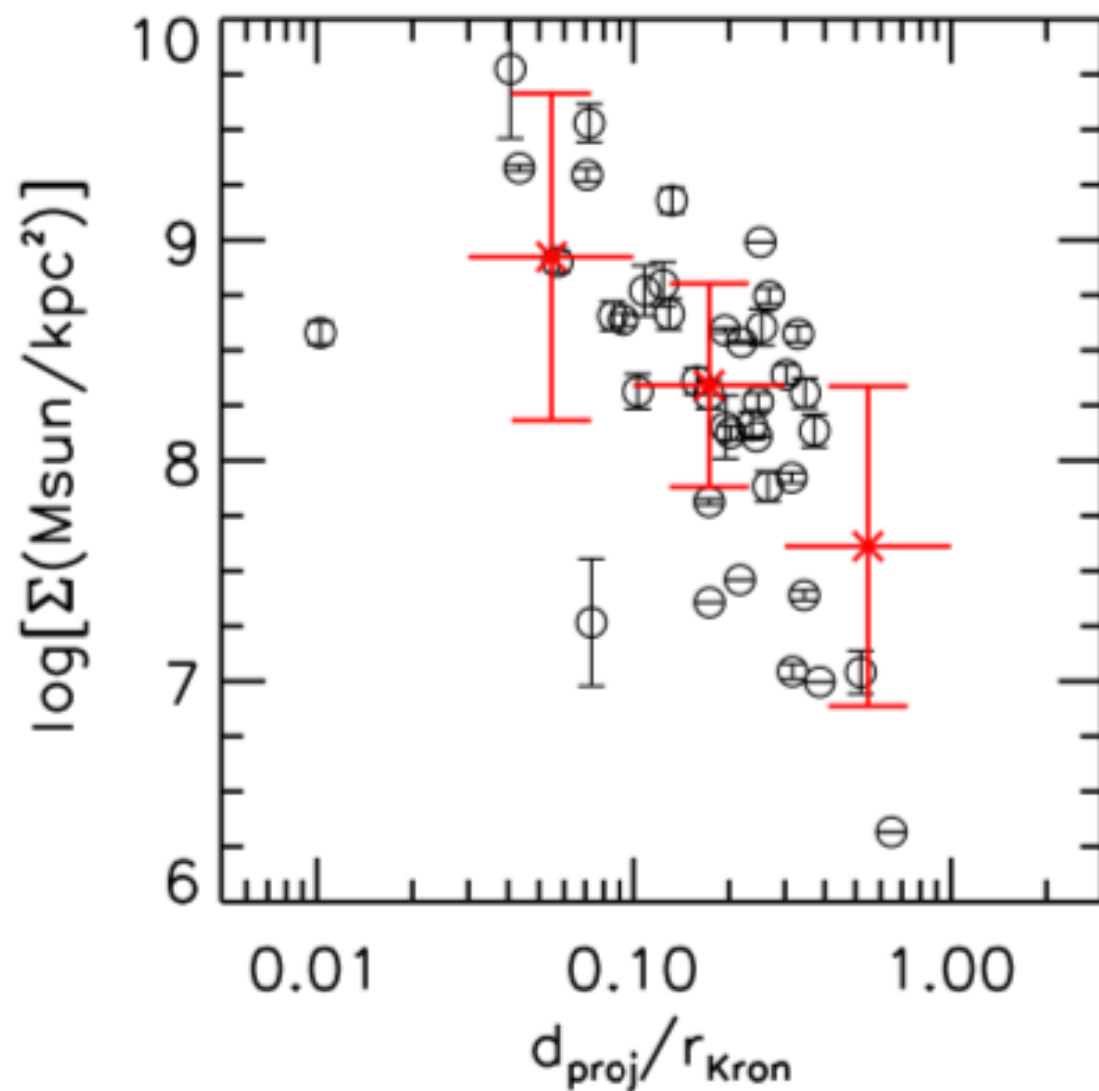
Bulge formation by gas accretion and clump migration

Clumps are older and denser closer to the galactic center

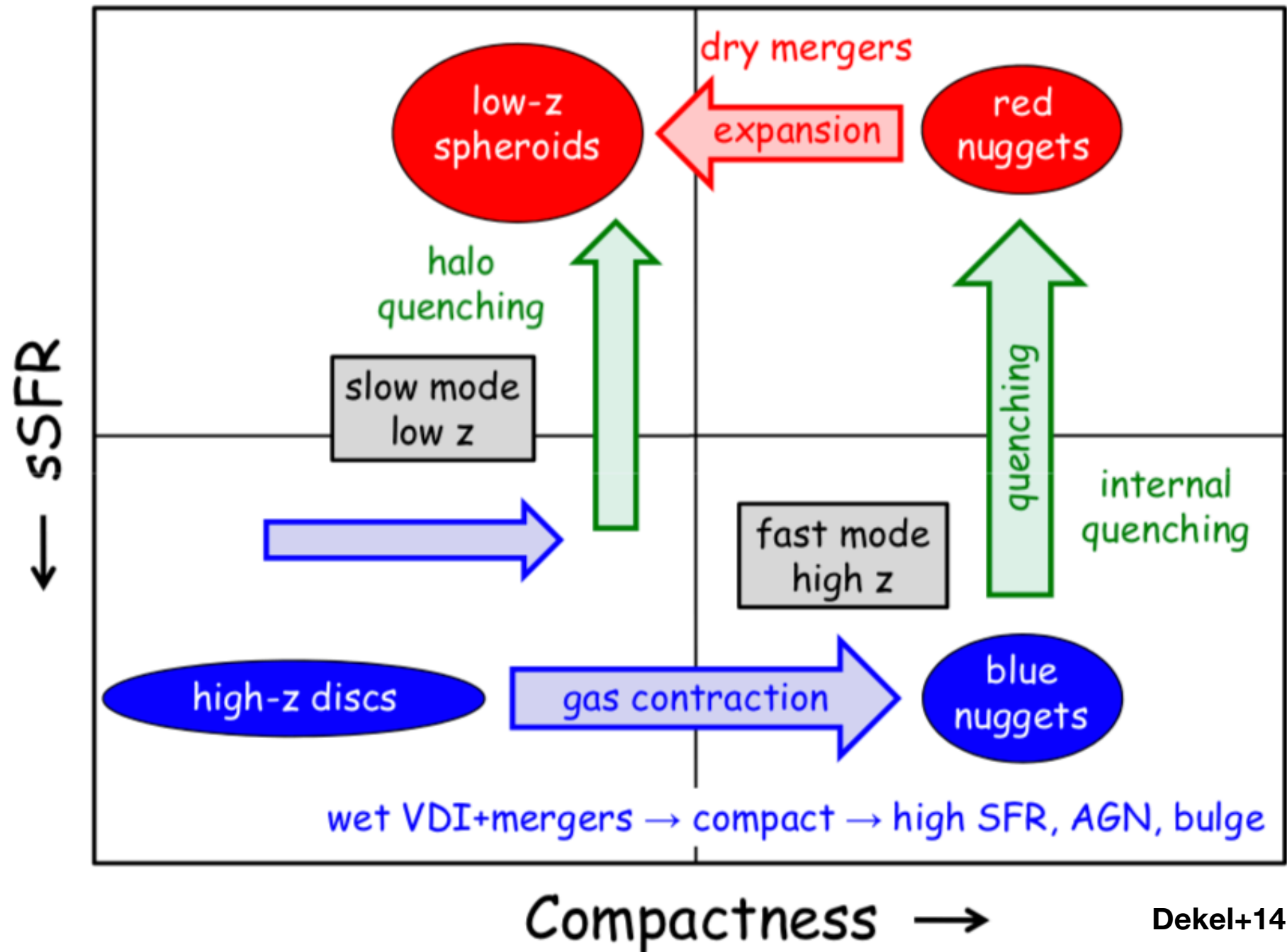


Bulge formation by gas accretion and clump migration

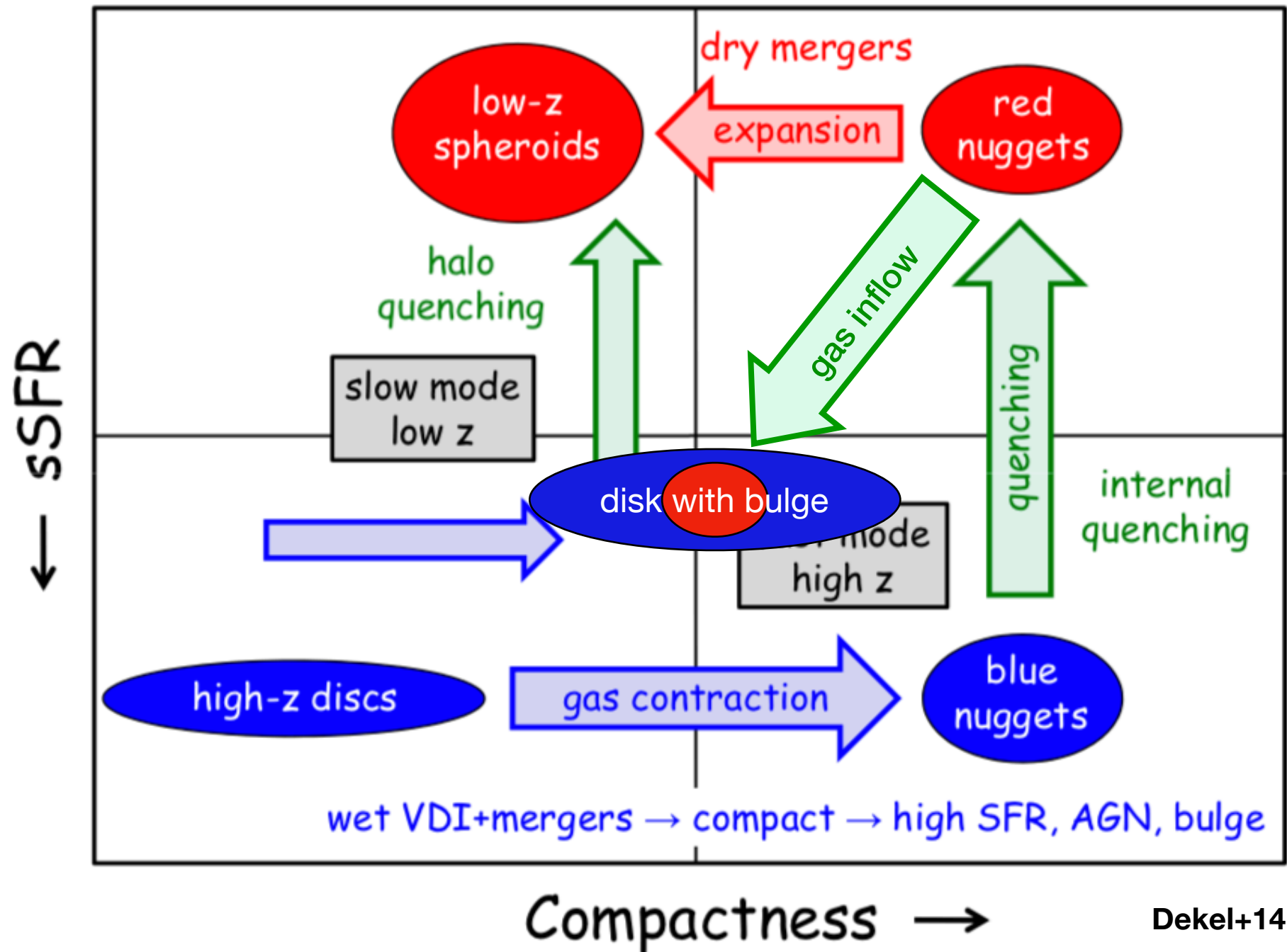
Clumps are older and denser closer to the galactic center



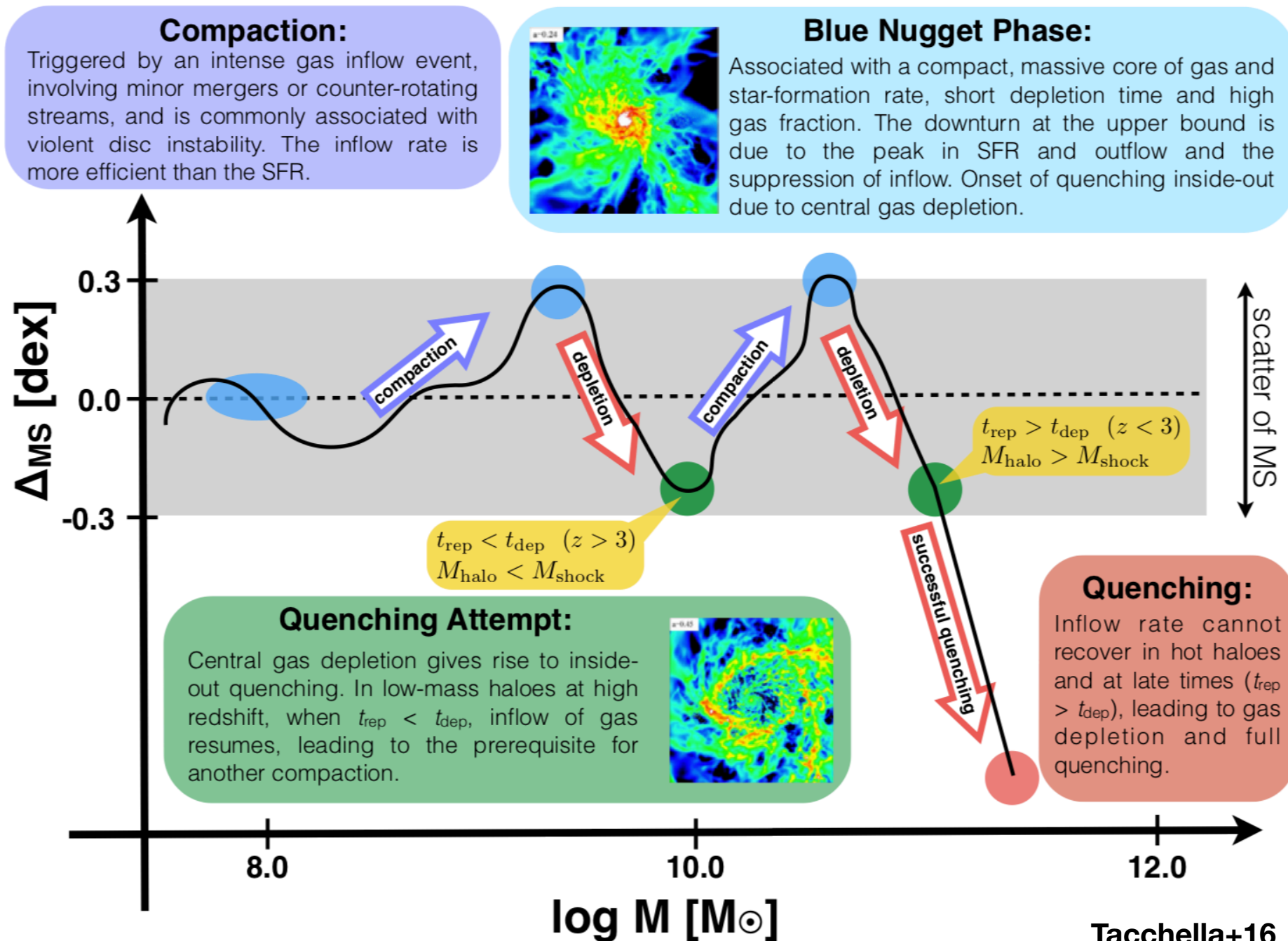
Bulge formation by wet disk contraction



Bulge formation by wet disk contraction

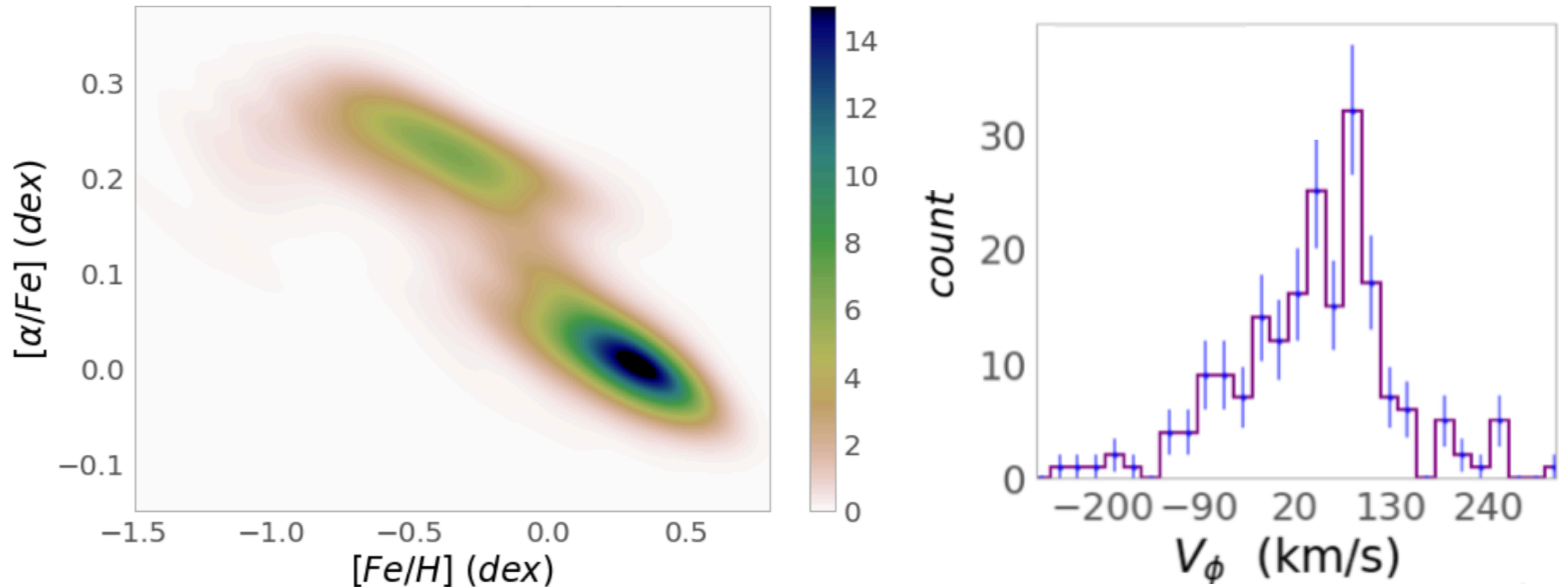


Bulge formation by wet disk contraction



The Milky Way

The galactic center is chemically older and has kinematic signatures of clump accretion

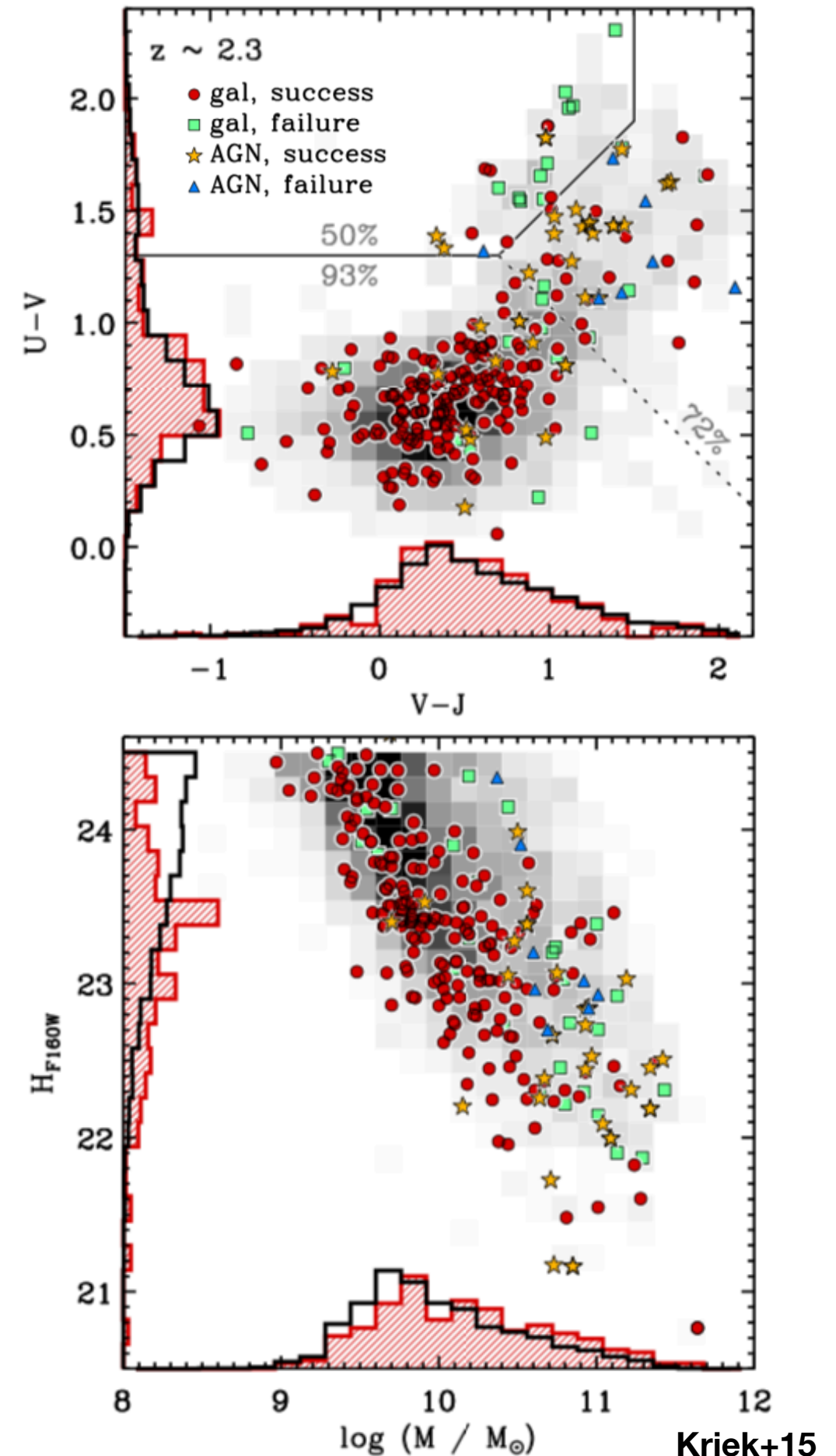


Queiroz+20

Bulge sample

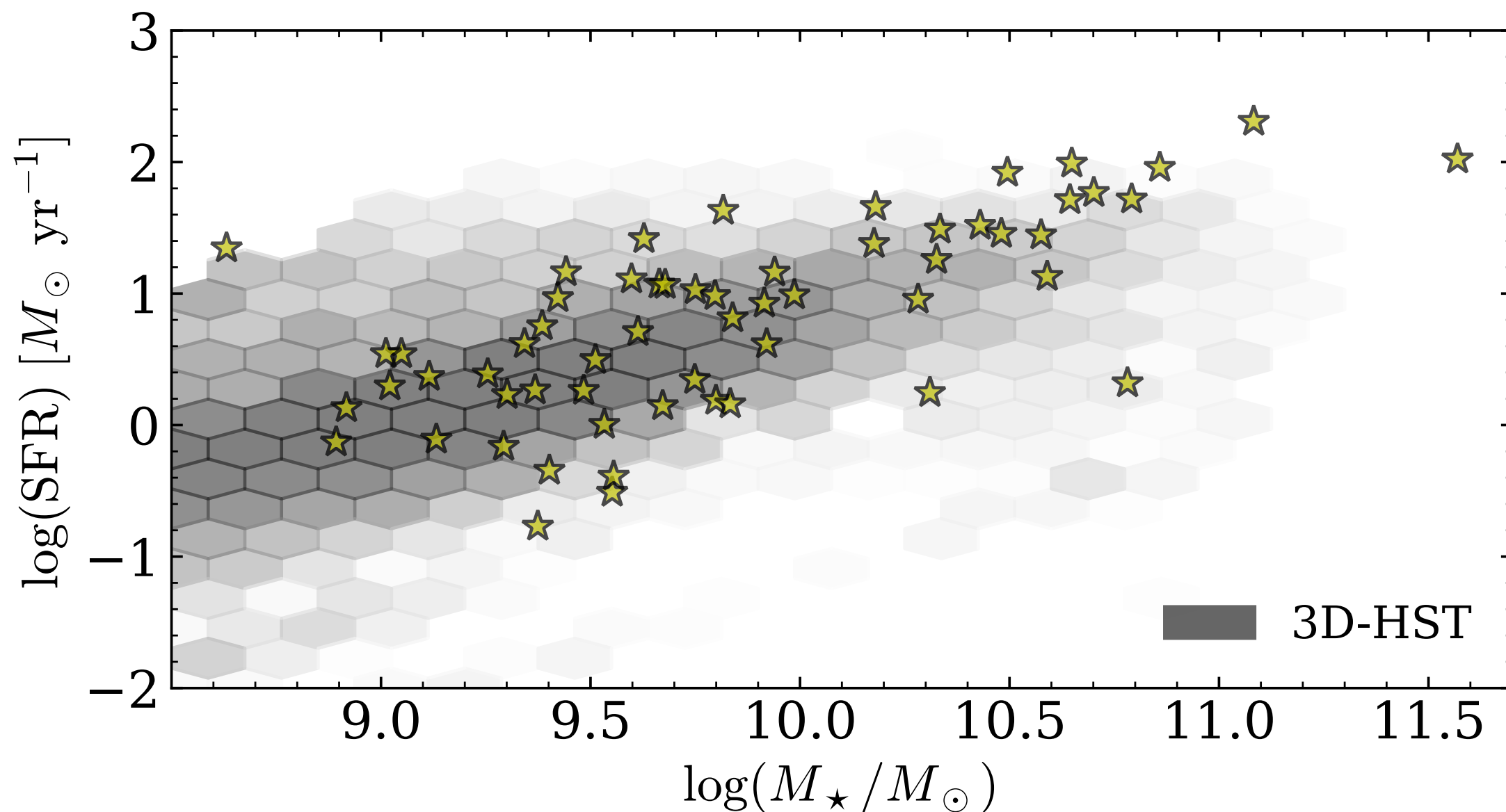
60 galaxies at $z \sim 2.3$ from MOSDEF

- Mostly galaxies in the middle of the SFR-M relation
- Broadband photometry from CANDELS/SHARDS in GOODS-N:
 - 9 HST bands, ground-based U - and K -band, *Spitzer*/IRAC bands
- H -, J -, and K -band spectra (redshifts and metallicities) from MOSDEF
- AGN removed with X-ray, IR, emission line diagnostics



Bulge Sample

Primarily located in middle of main sequence



Introduction

Background

Existing theories of
galaxy structural
component formation

Sample selection

Analysis

Bulge detection and
decompositions

SED fitting: *Prospector*

Dealing with unresolved
photometry

Results

Detections

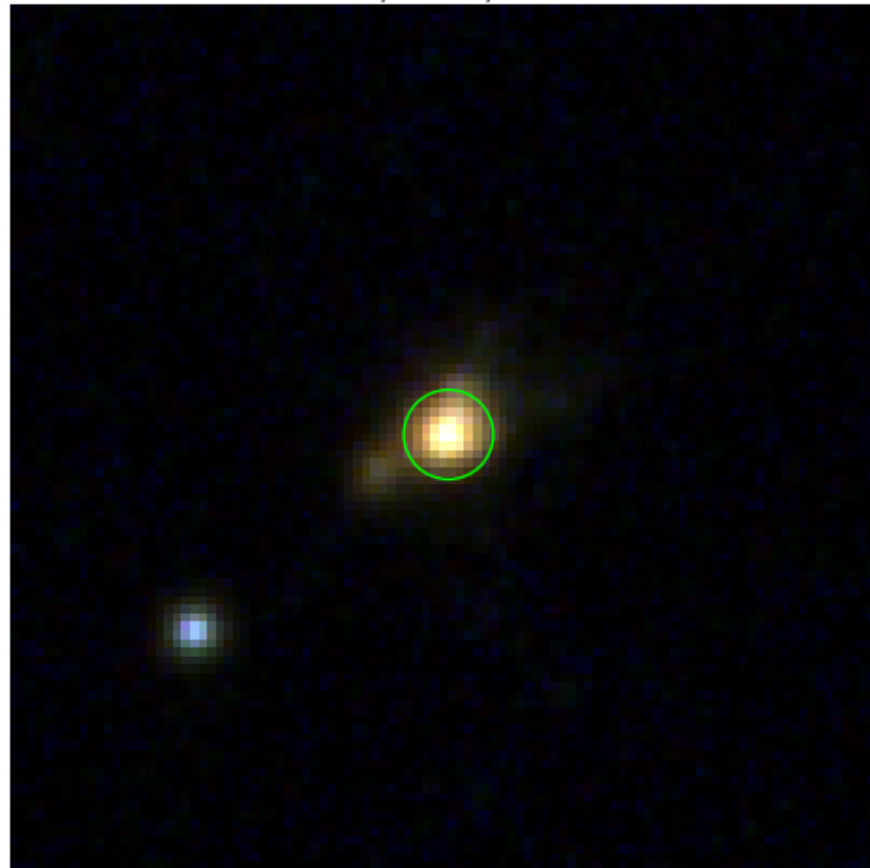
Star formation histories
and bulge formation

Future tests and analyses

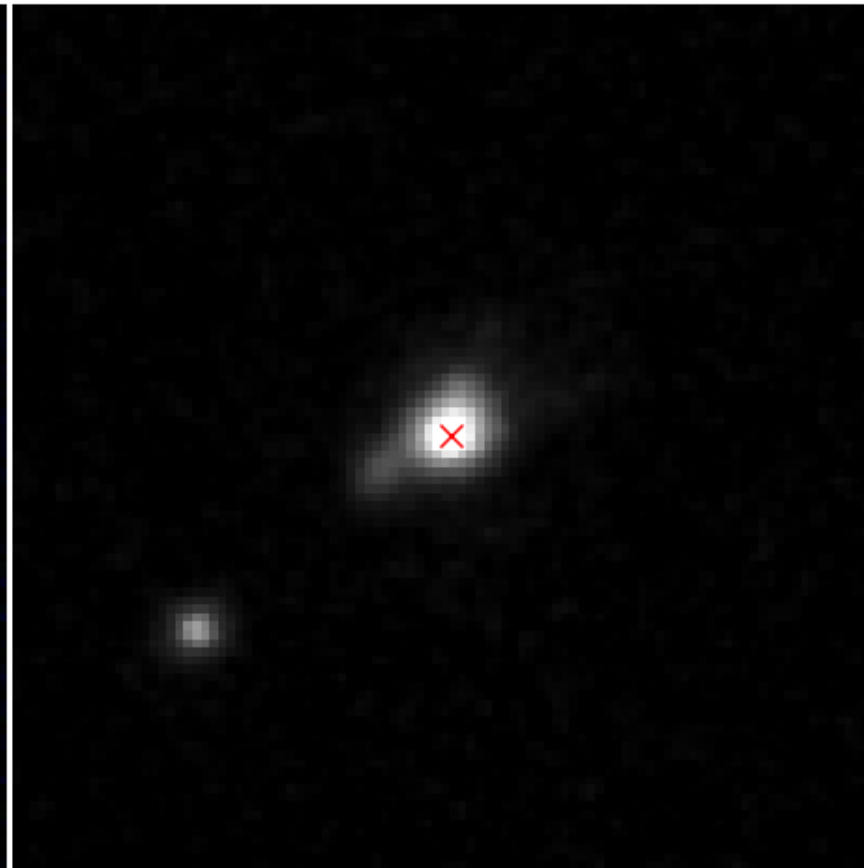
Bulge decomposition

Bulges are selected with $z-H$ colors

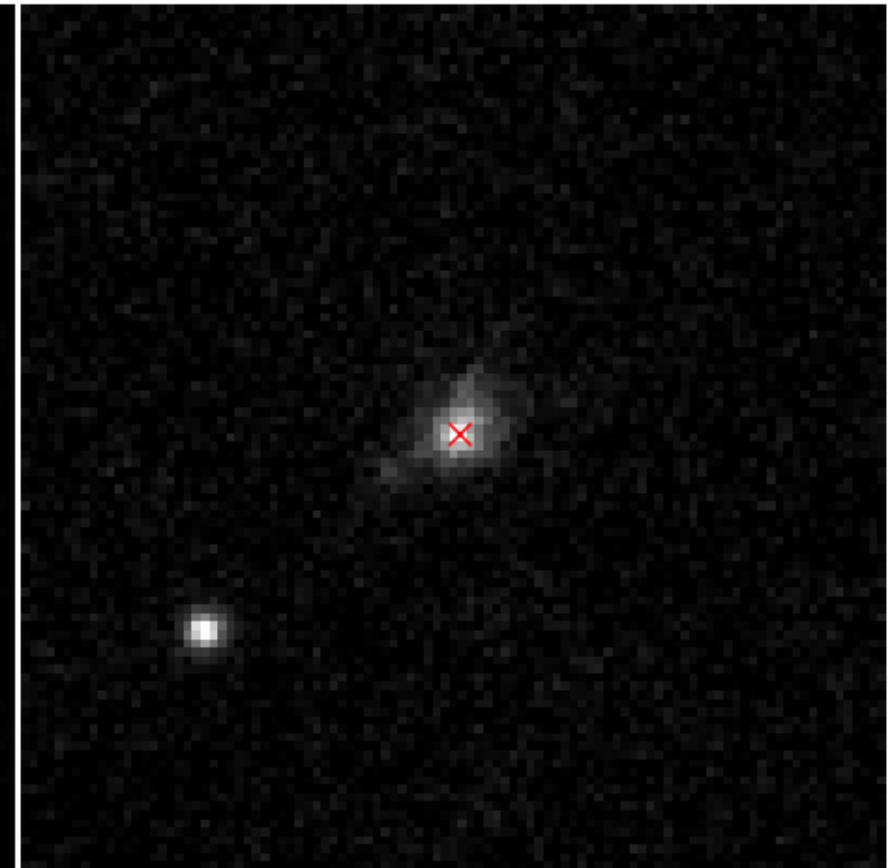
$f_{160}/f_{125}/f_{850}$



f_{160}

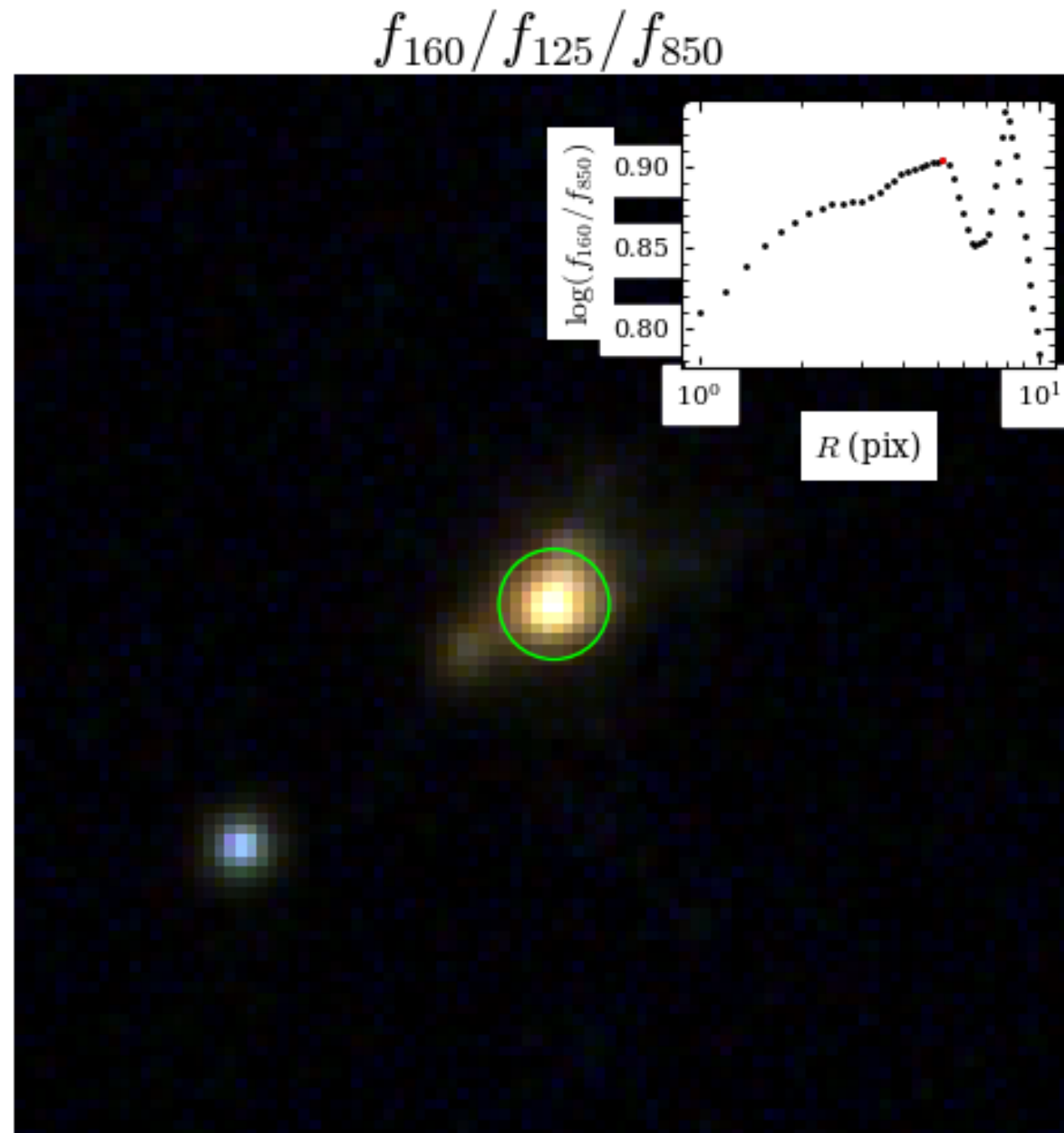


f_{850}



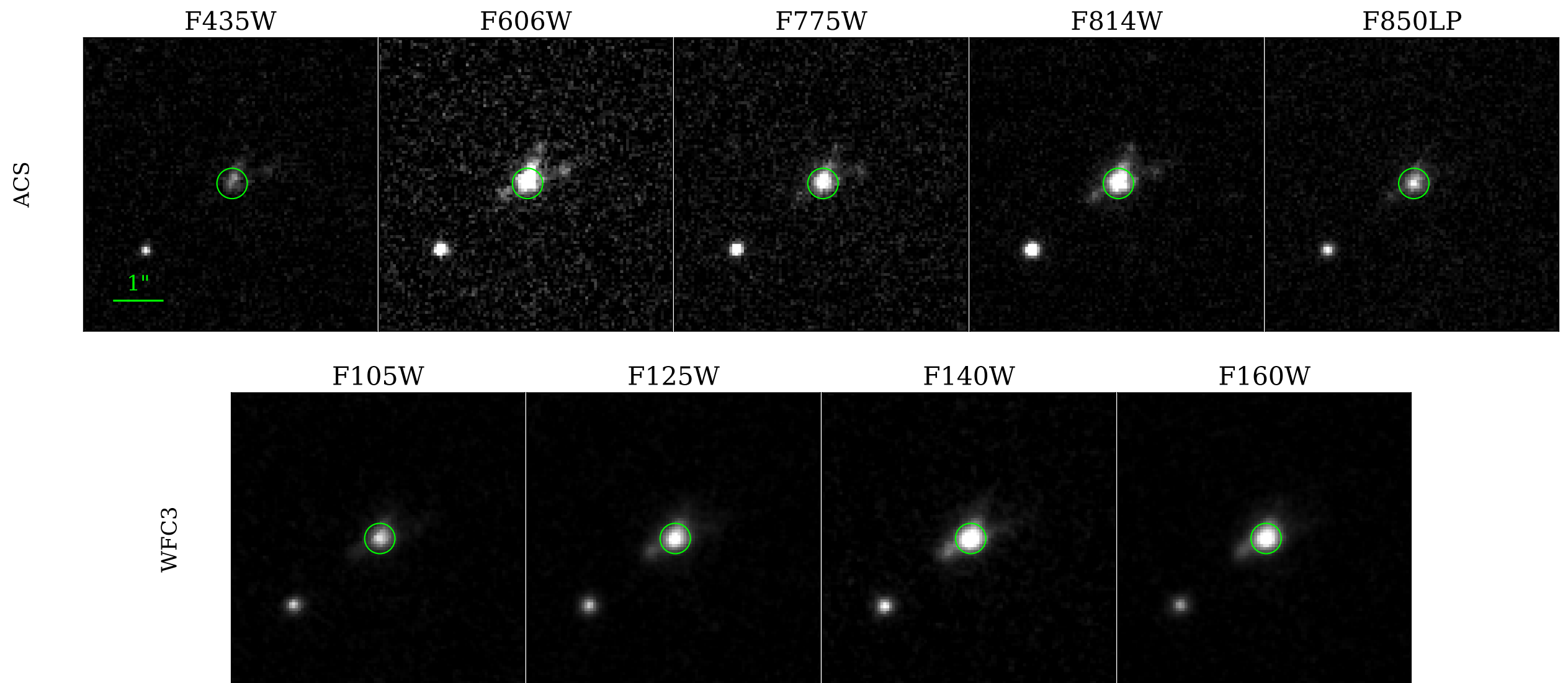
Bulge decomposition

Bulges are selected with $z-H$ colors



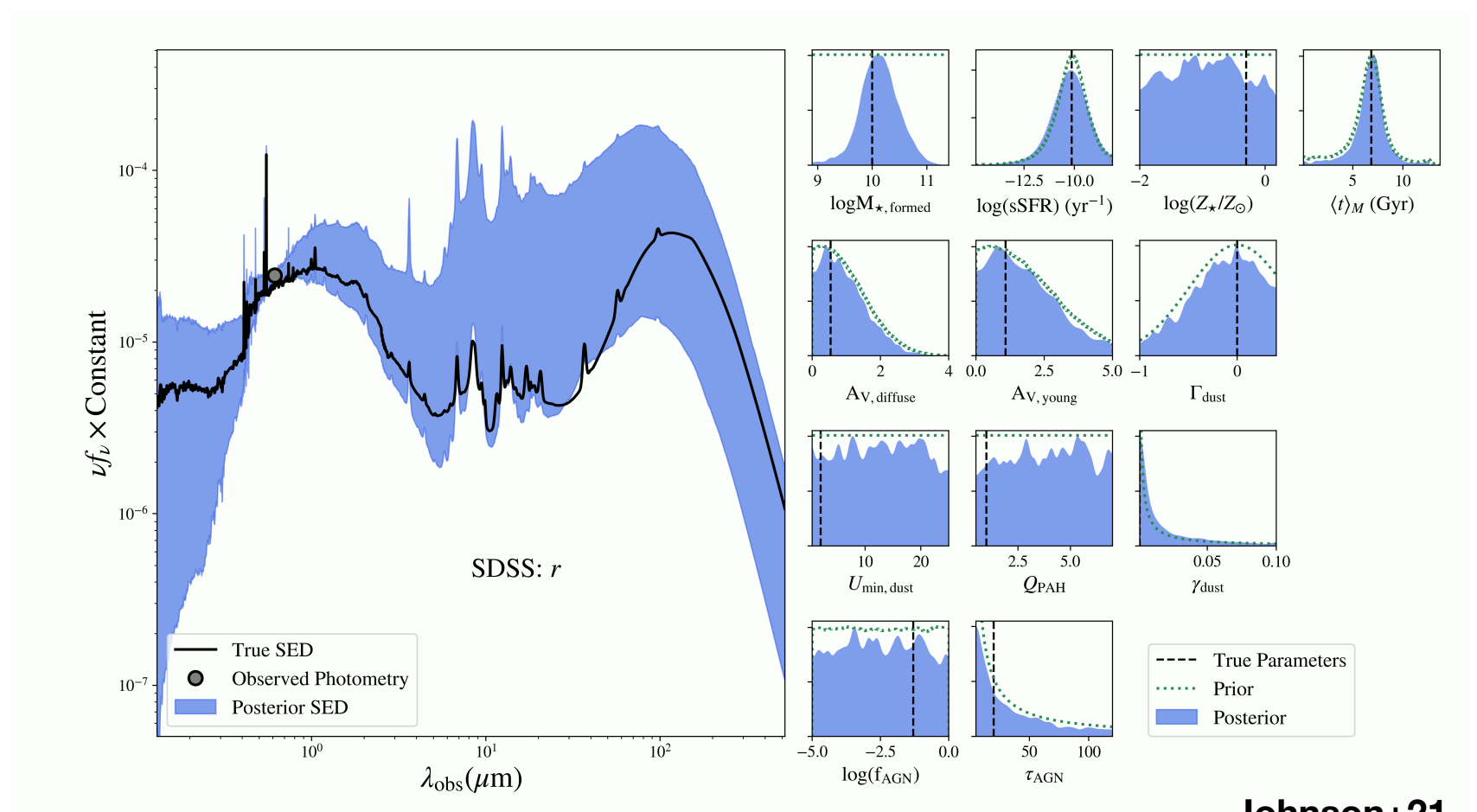
Bulge decomposition

Photometry measured using same aperture in all filters



Prospector

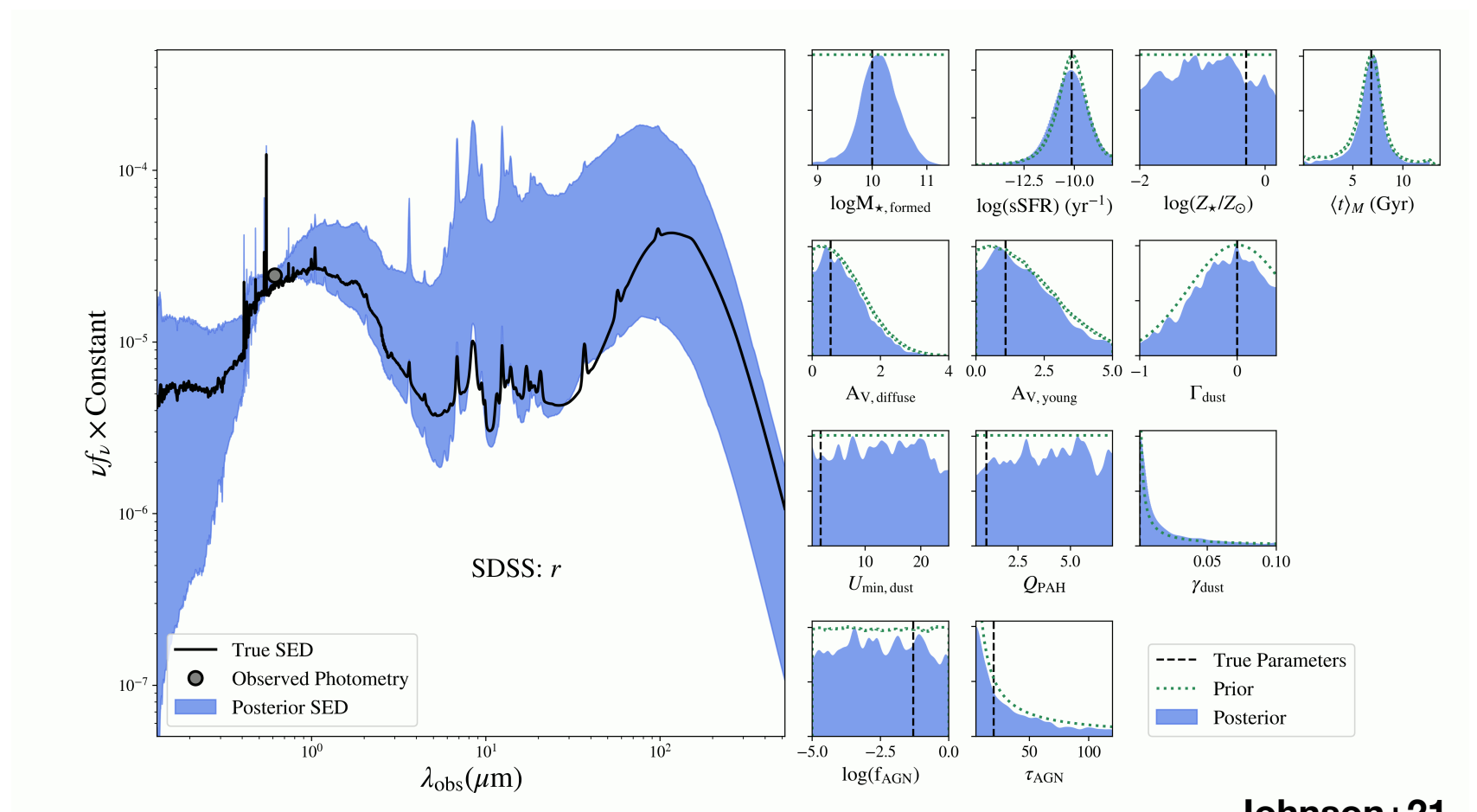
1. Bayesian forward-modeling and Monte-Carlo sampling
2. Gridless SED modeling
3. Very flexible



Johnson+21

Prospector

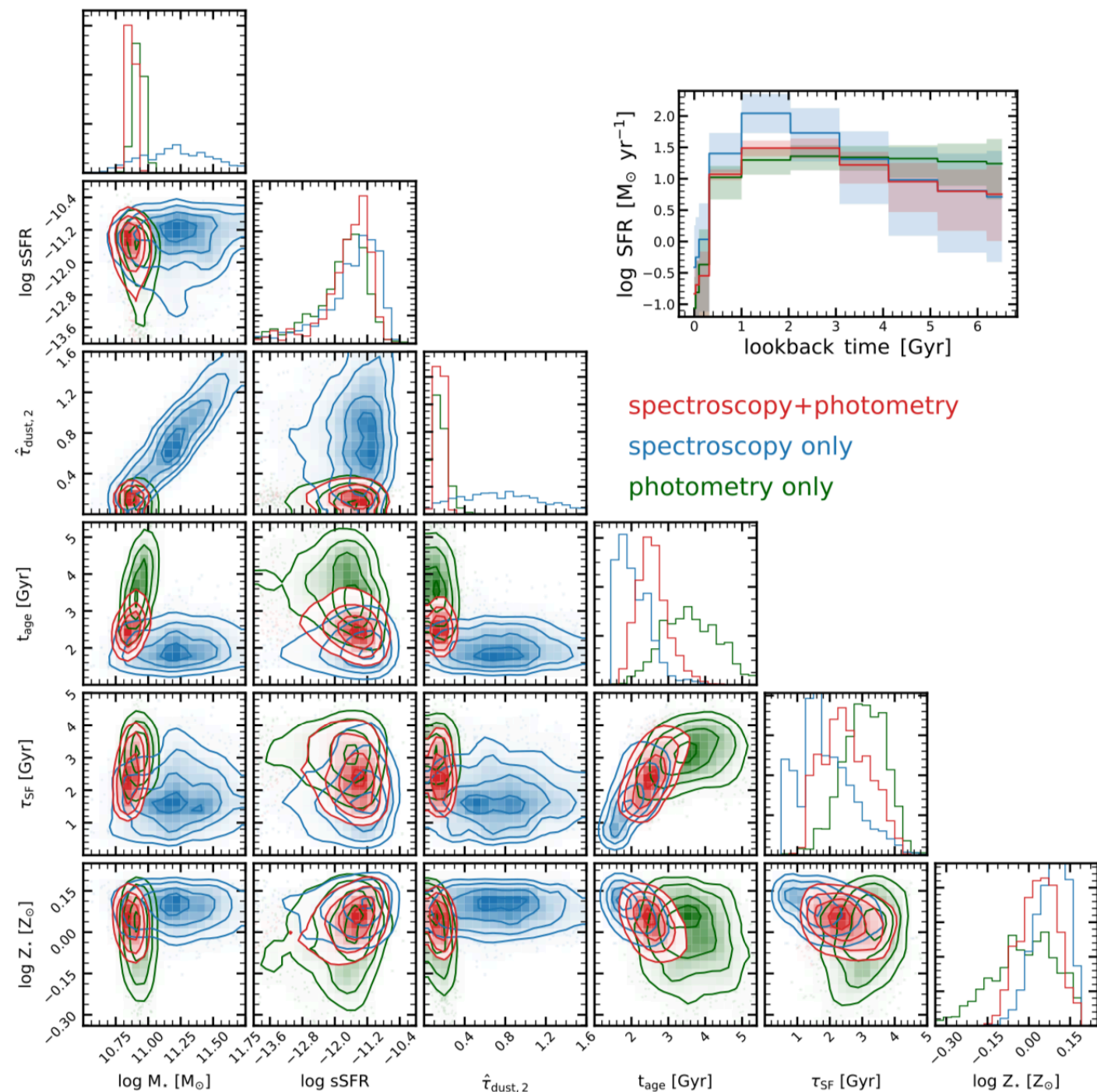
1. Bayesian forward-modeling and Monte-Carlo sampling
2. Gridless SED modeling
3. Very flexible



Johnson+21

Priors are important

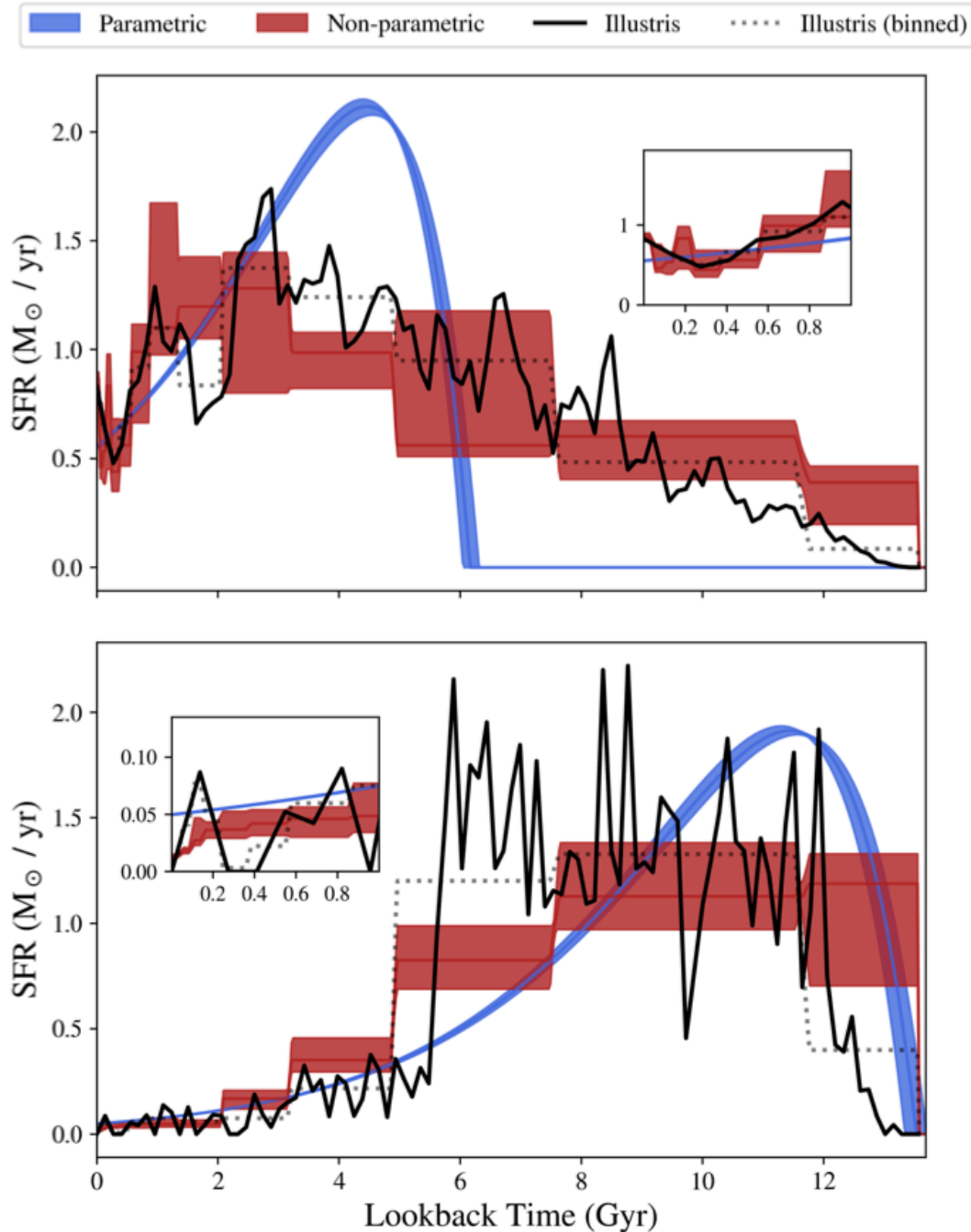
Spectroscopy most useful in constraining the age/metallicity



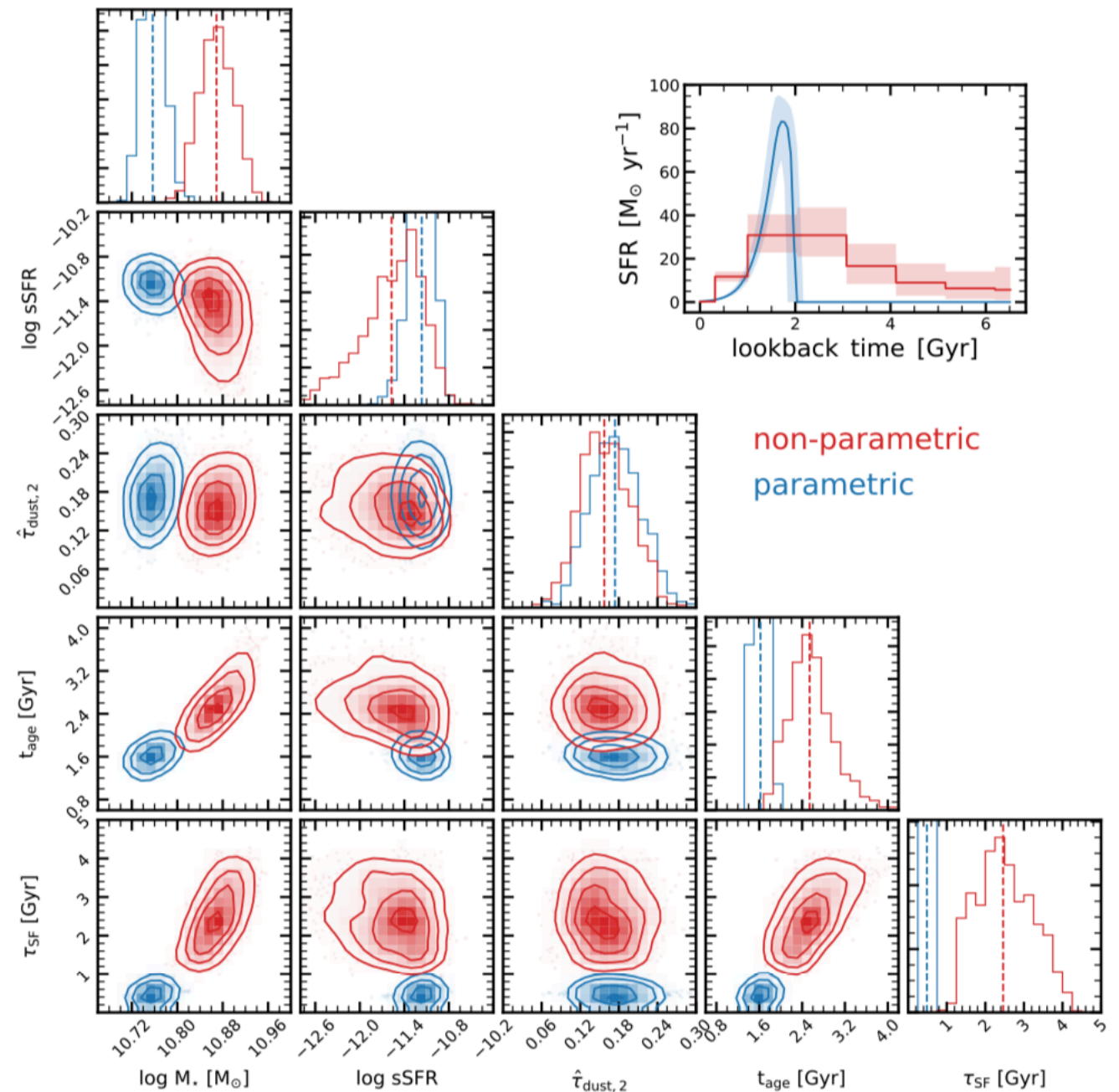
Tacchella+21

Priors are important

Parametric SFHs can dramatically differ from non-parametric SFHs



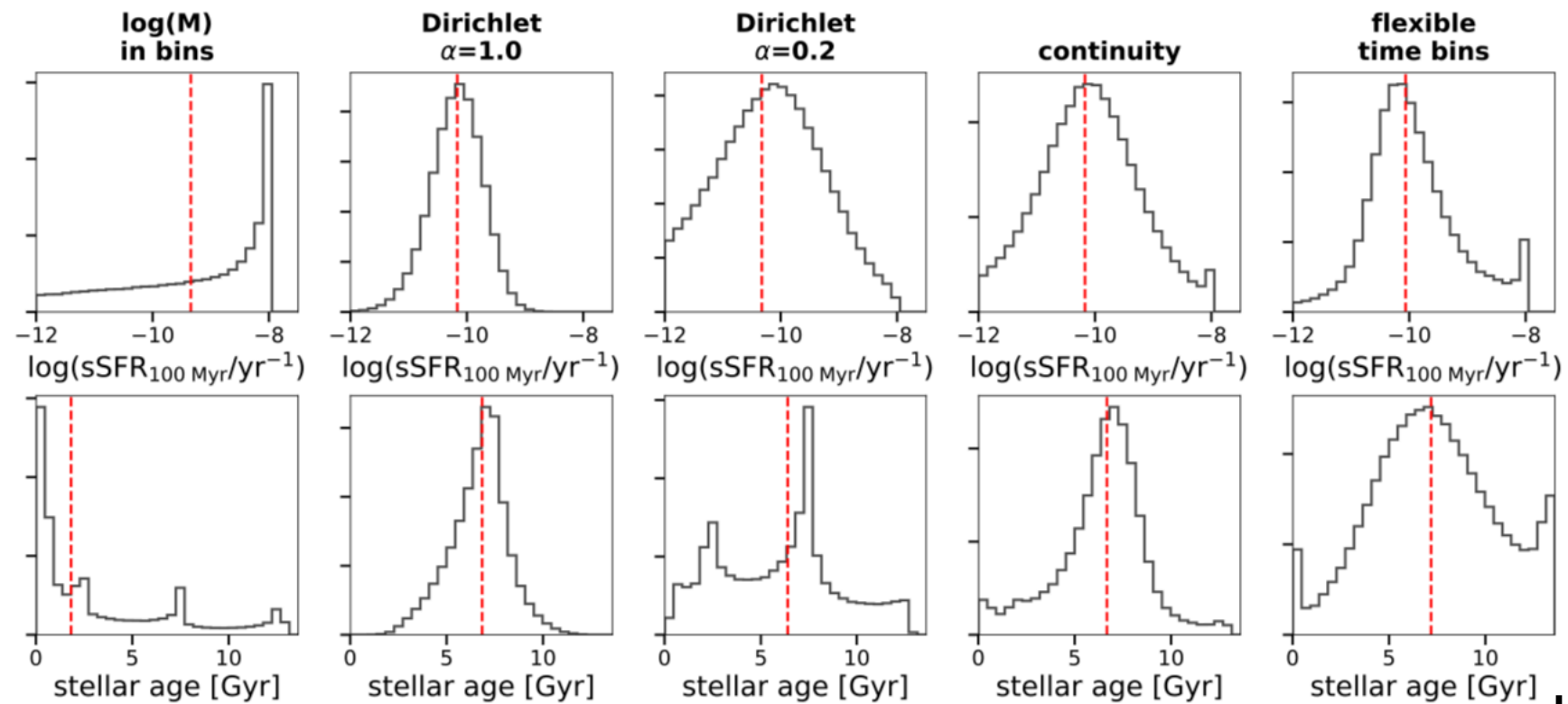
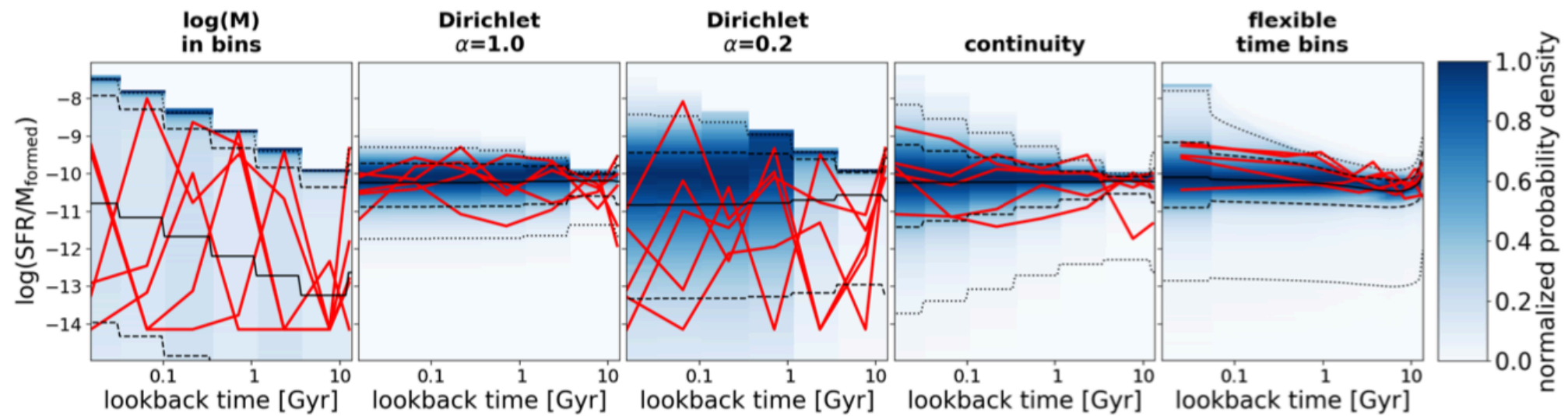
Johnson+21



Tacchella+21

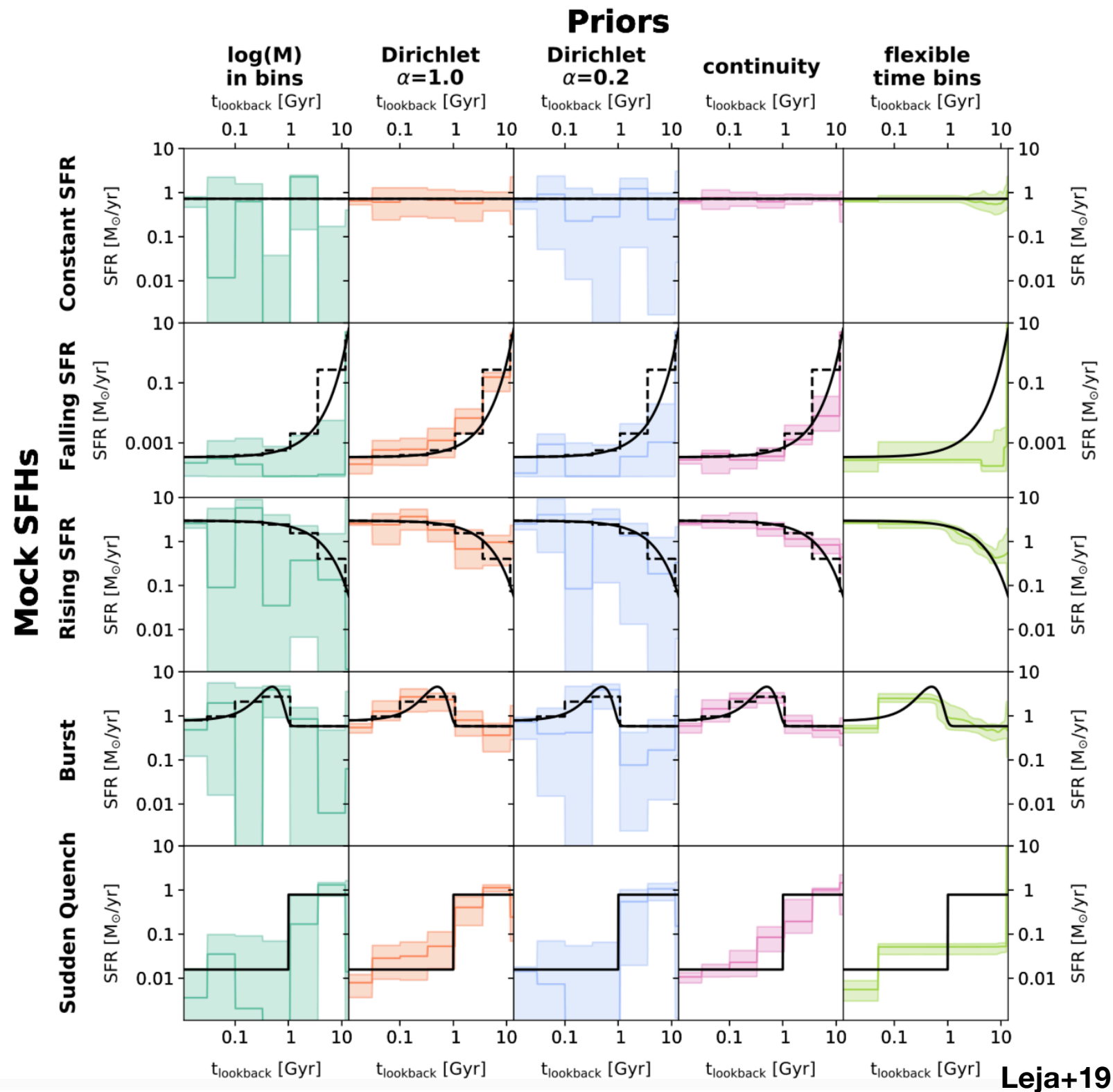
Priors are important

Choice of non-parametric prior can also impact SFH significantly



Leja+19

Priors are important



Prospector ingredients

Separately run on bulge, disk and total galaxy

Photometry:

- All HST bands, *K*-band, IRAC (*U*-band for total galaxy)

Model:

- Non-parametric SFH (7/5 time bins), Chabrier IMF, dust and nebular emission

Free Parameters:

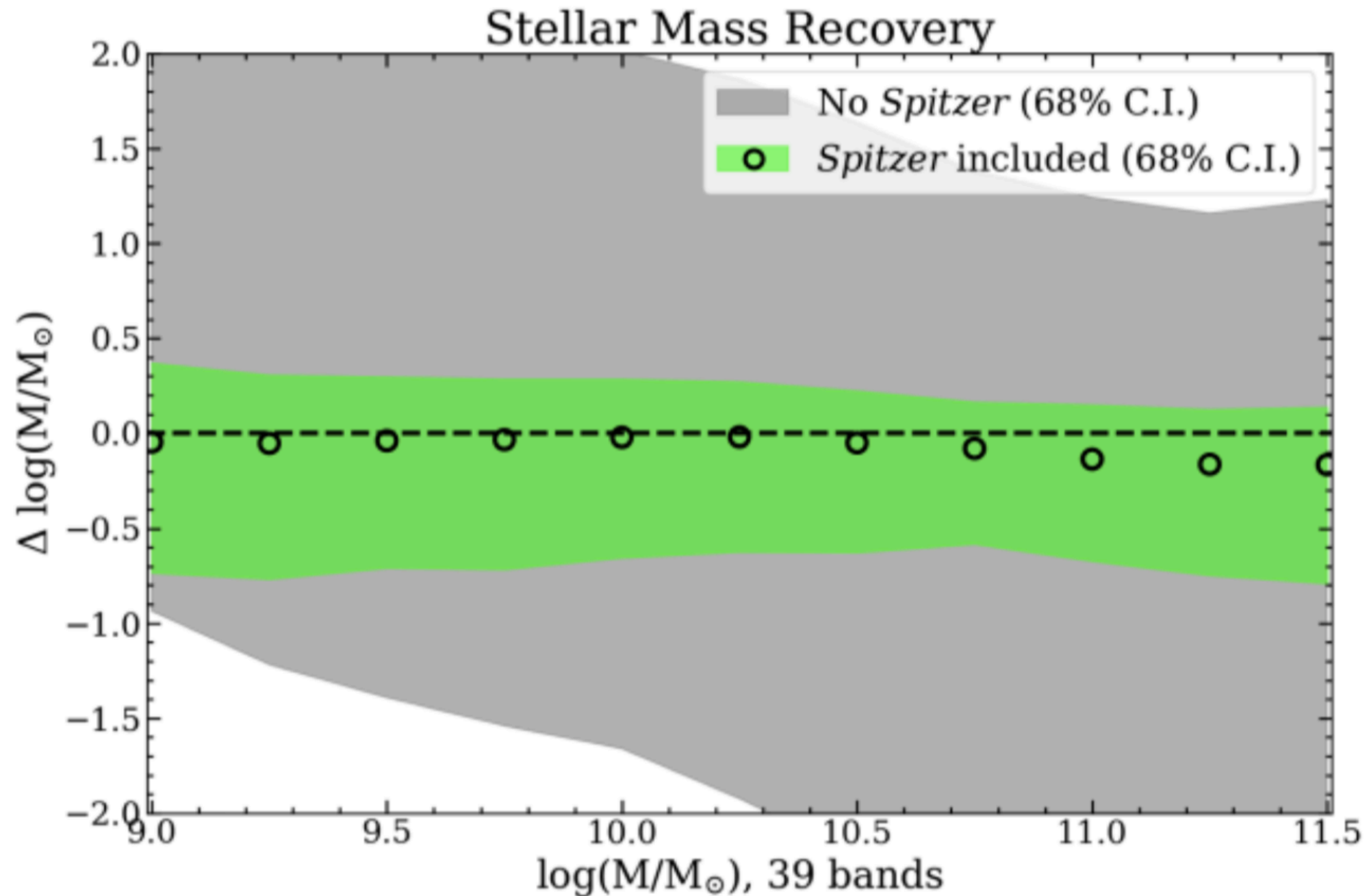
- Stellar metallicity ($\log Z_*$), *V*-band optical depth (τ_V), ionization parameter (U_{neb}), total mass formed (M_F), ratio of SFRs ($\Delta \log(\text{SFR})$)

Priors:

- Gaussian prior on $\log Z_*$, continuity prior on SFH

Prospector ingredients

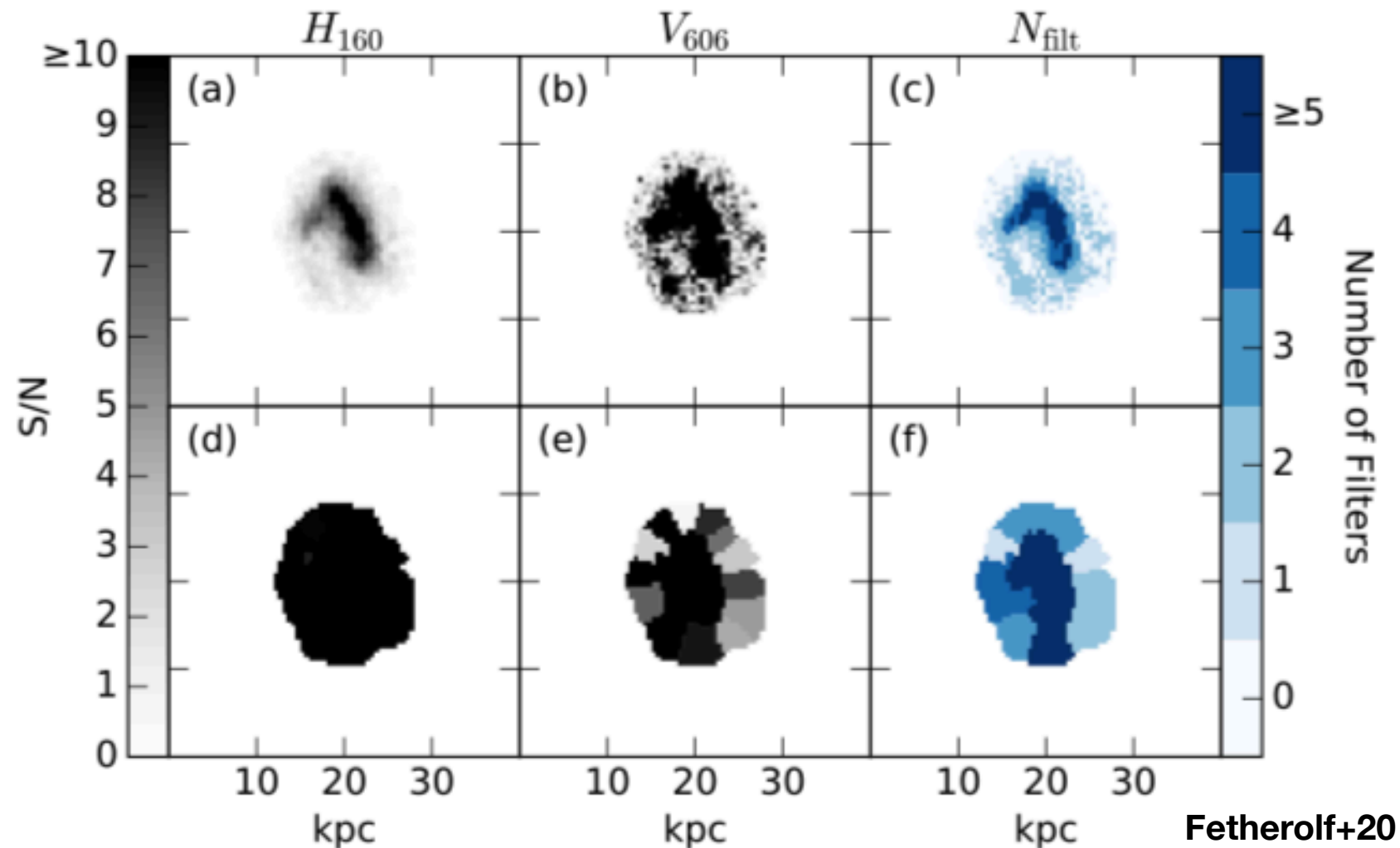
IRAC is extremely important in SED fitting



Dealing with IRAC photometry

IRAC photometry can be determined iteratively for a two component system

Reason behind simple decomposition vs pixel by pixel or Voronoi binning



Dealing with IRAC photometry

Dealing with IRAC photometry

1. Fit HST photometry only for bulge and disk
 - ▶ Only use 5 time bins

Dealing with IRAC photometry

1. Fit HST photometry only for bulge and disk
 - ▶ Only use 5 time bins
2. Correct K /IRAC from SED predictions using F160W:

$$f_{x,\text{corr}}(\lambda) = f_{x,\text{MAP}}(\lambda) \left(\frac{f_{x,\text{obs}}(\text{F160W})}{f_{x,\text{MAP}}(\text{F160W})} \right)$$

Dealing with IRAC photometry

1. Fit HST photometry only for bulge and disk

▶ Only use 5 time bins

2. Correct $K/IRAC$ from SED predictions using F160W:

$$f_{x,\text{corr}}(\lambda) = f_{x,\text{MAP}}(\lambda) \left(\frac{f_{x,\text{obs}}(\text{F160W})}{f_{x,\text{MAP}}(\text{F160W})} \right)$$

3. Scale $f_{x,\text{corr}}(\lambda)$ by total $K/IRAC$ flux ($f_{\text{obs}}(\lambda)$):

$$f'_x(\lambda) = f_{x,\text{corr}}(\lambda) \left(\frac{f_{\text{obs}}(\lambda)}{\sum_x f_{x,\text{corr}}(\lambda)} \right)$$

Dealing with IRAC photometry

1. Fit HST photometry only for bulge and disk

▶ Only use 5 time bins

2. Correct $K/IRAC$ from SED predictions using F160W:

$$f_{x,\text{corr}}(\lambda) = f_{x,\text{MAP}}(\lambda) \left(\frac{f_{x,\text{obs}}(\text{F160W})}{f_{x,\text{MAP}}(\text{F160W})} \right)$$

3. Scale $f_{x,\text{corr}}(\lambda)$ by total $K/IRAC$ flux ($f_{\text{obs}}(\lambda)$):

$$f'_x(\lambda) = f_{x,\text{corr}}(\lambda) \left(\frac{f_{\text{obs}}(\lambda)}{\sum_x f_{x,\text{corr}}(\lambda)} \right)$$

4. Refit components with $f'_x(\lambda)$ for observed $K/IRAC$ flux and repeat

Dealing with IRAC photometry

1. Fit HST photometry only for bulge and disk

▶ Only use 5 time bins

2. Correct $K/IRAC$ from SED predictions using F160W:

$$f_{x,\text{corr}}(\lambda) = f_{x,\text{MAP}}(\lambda) \left(\frac{f_{x,\text{obs}}(\text{F160W})}{f_{x,\text{MAP}}(\text{F160W})} \right)$$

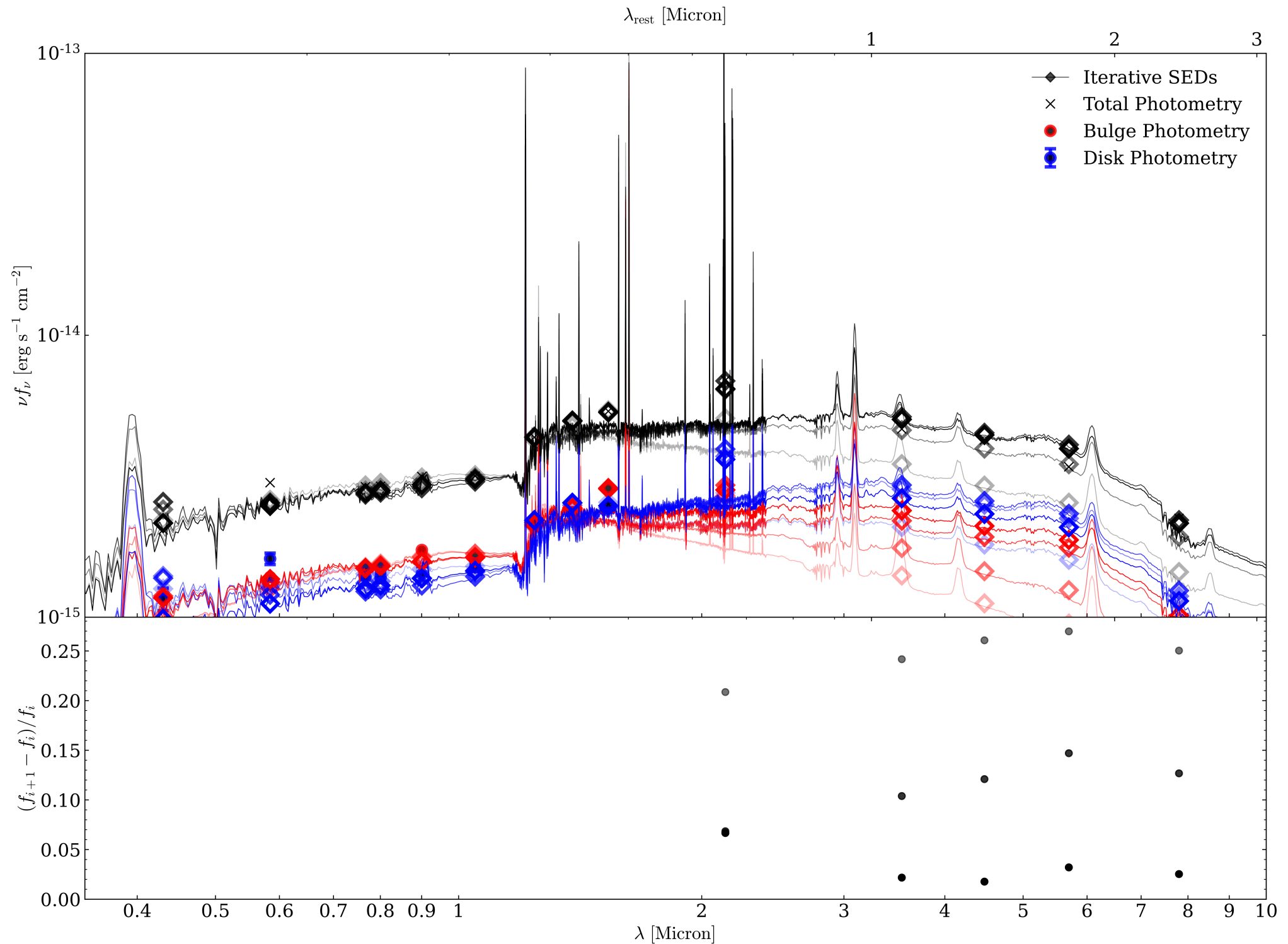
3. Scale $f_{x,\text{corr}}(\lambda)$ by total $K/IRAC$ flux ($f_{\text{obs}}(\lambda)$):

$$f'_x(\lambda) = f_{x,\text{corr}}(\lambda) \left(\frac{f_{\text{obs}}(\lambda)}{\sum_x f_{x,\text{corr}}(\lambda)} \right)$$

4. Refit components with $f'_x(\lambda)$ for observed $K/IRAC$ flux and repeat

5. Stop when $\Delta f'_x(\lambda)/f'_x(\lambda) < 0.05$ for all but one band

Dealing with IRAC photometry



Introduction

Background

Existing theories of
galaxy structural
component formation

Sample selection

Analysis

Bulge detection and
decompositions

SED fitting: *Prospector*

Dealing with unresolved
photometry

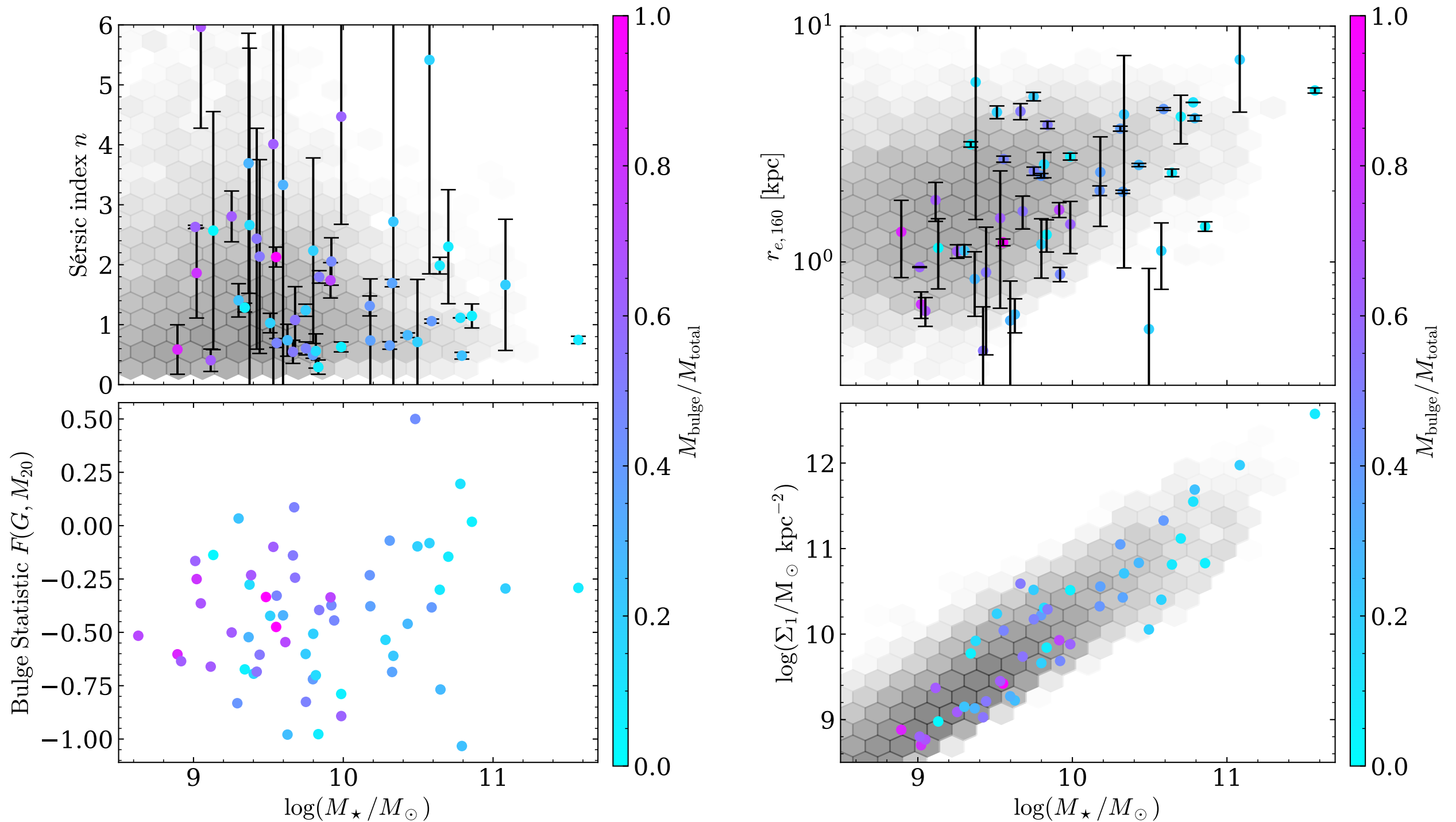
Results

Detections

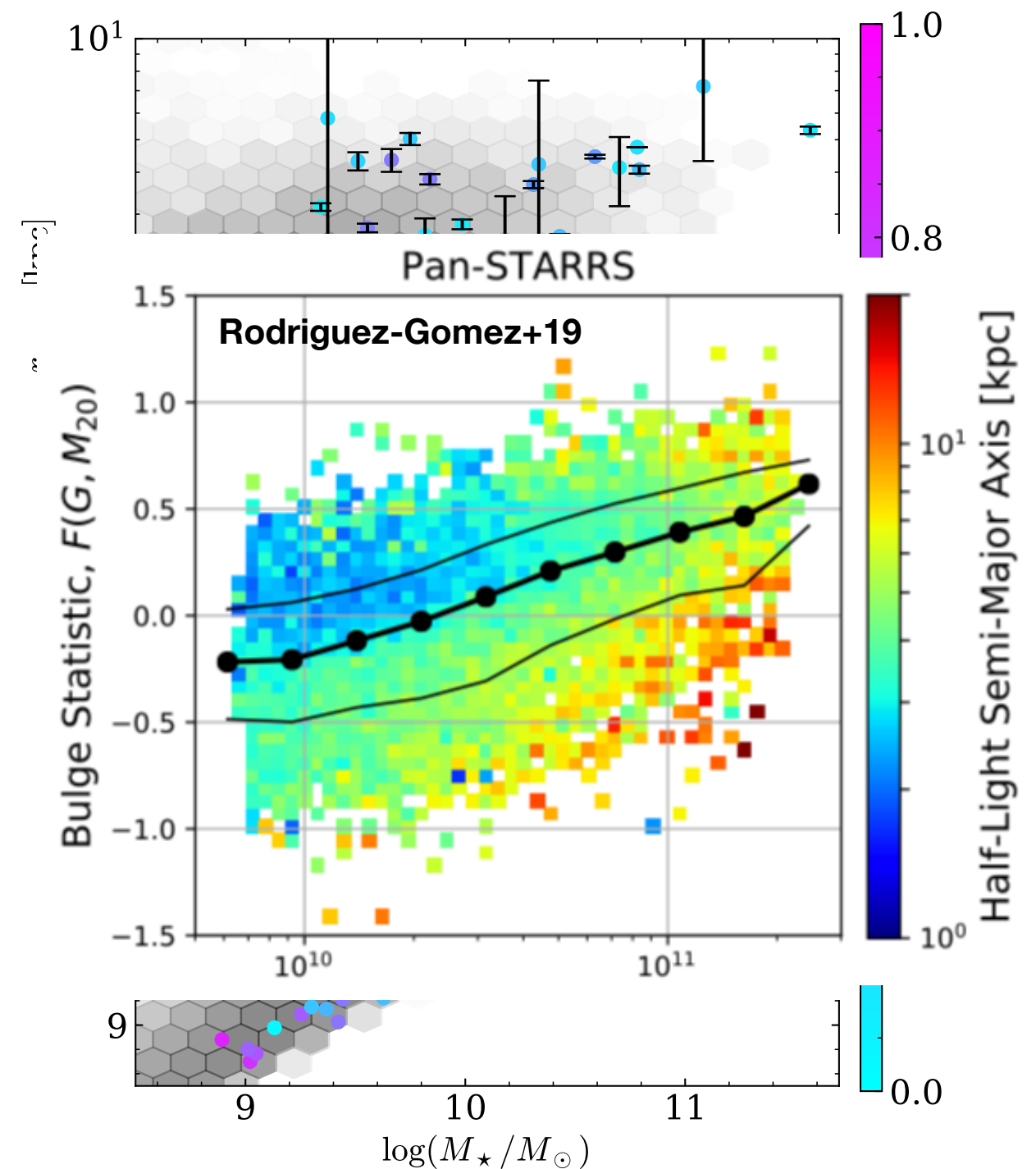
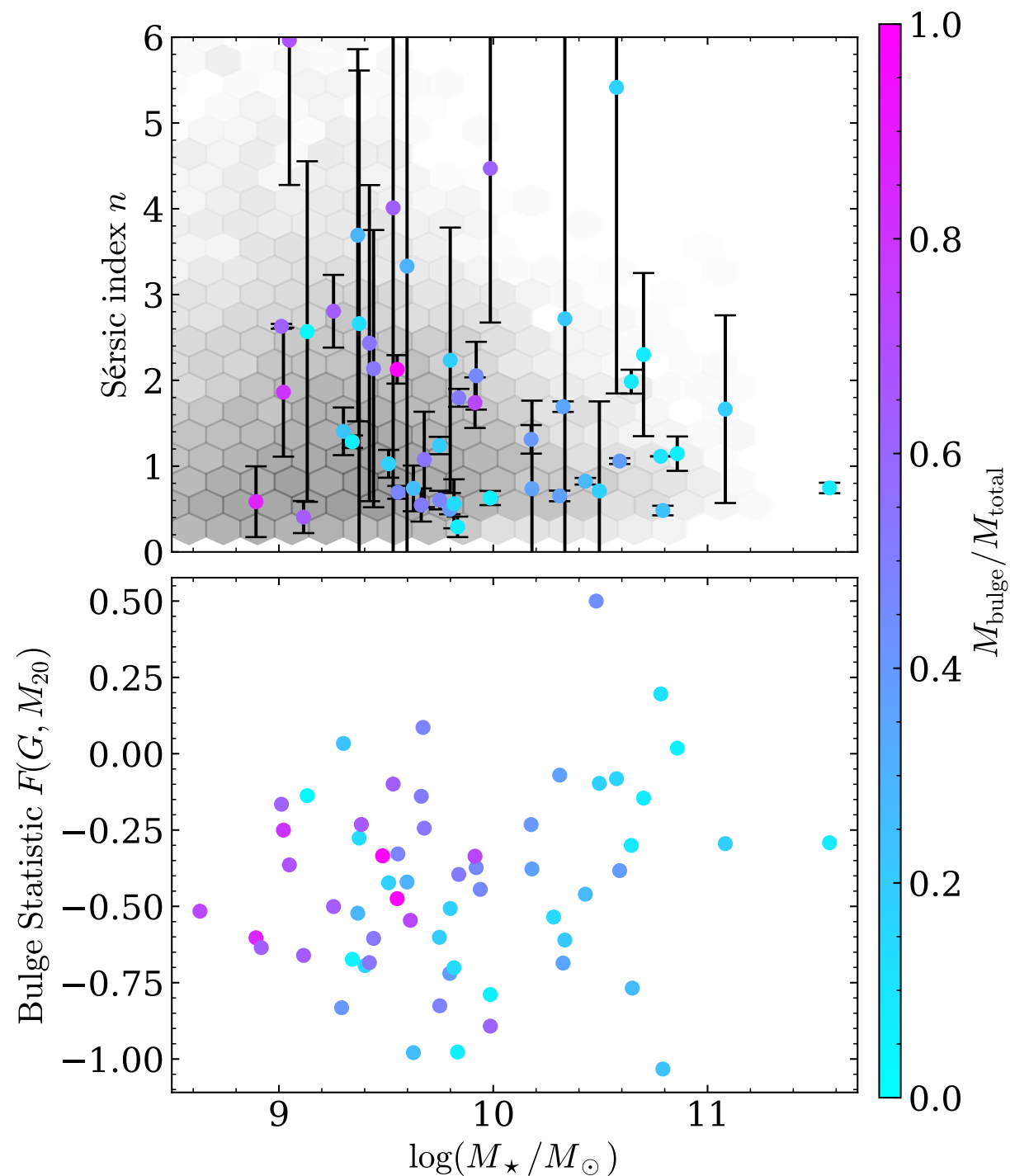
Star formation histories
and bulge formation

Future tests and analyses

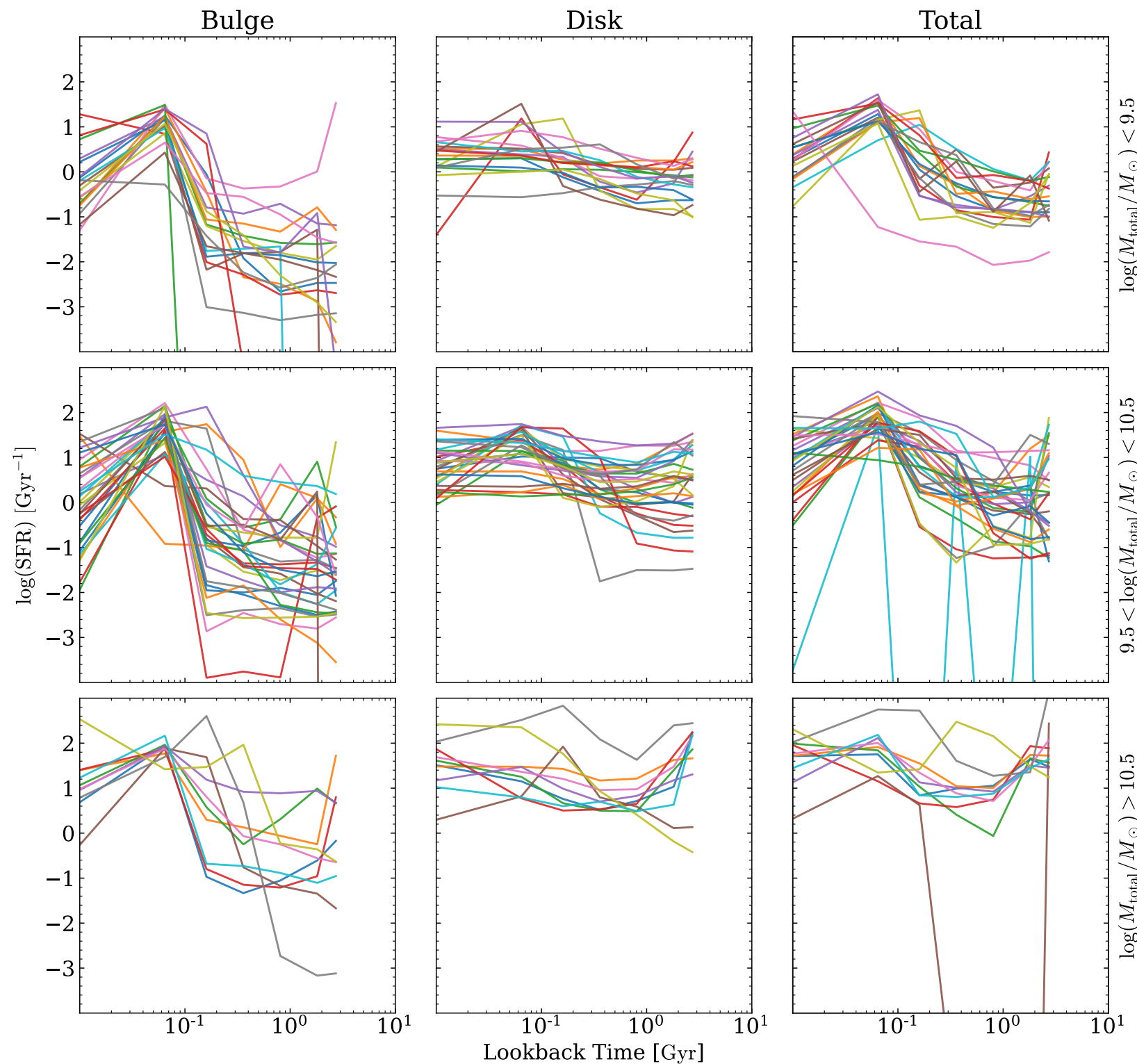
Structural comparisons



Structural comparisons



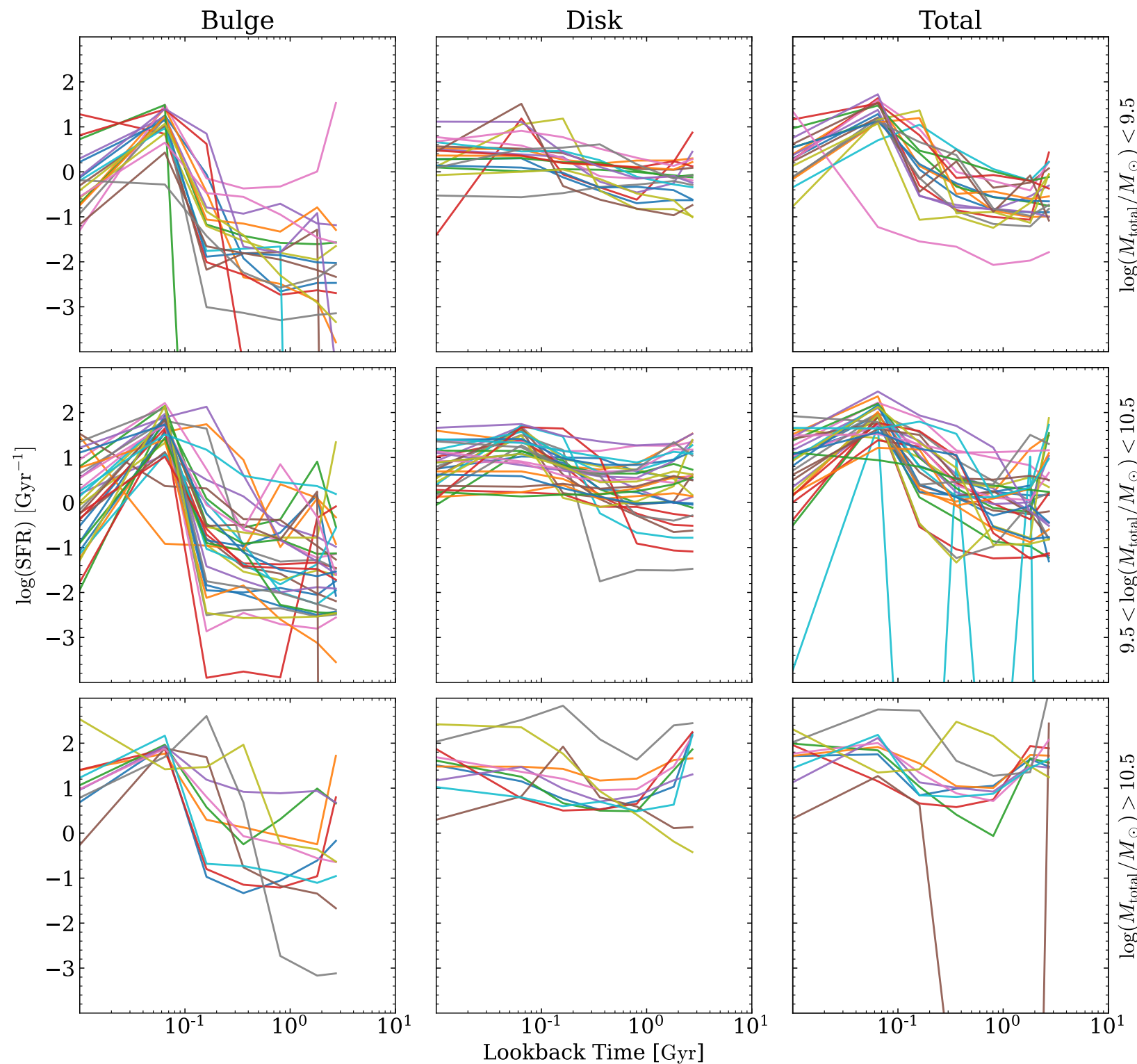
Star formation histories



Sharper peaks in SFH, rising total SFH

Less peaked SFH, more constant total SFH

Star formation histories



Sharper peaks in SFH, rising total SFH

Sub-massive galaxies: rapid formation of bulge later

Massive galaxies: inside out formation

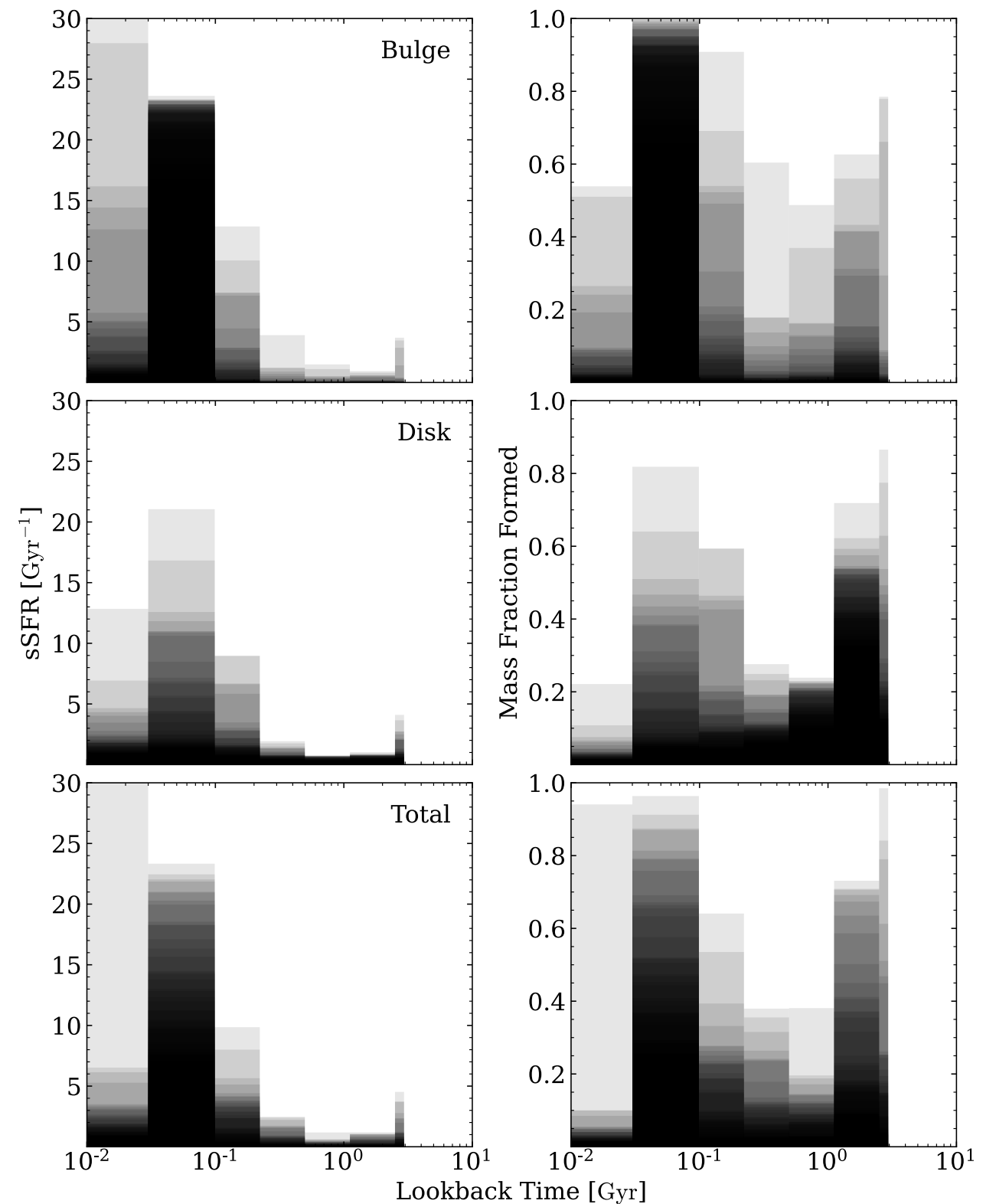
Less peaked SFH, more constant total SFH

Star formation histories

Sharp peak in bulge SFH implies bulge formed in a burst of star formation

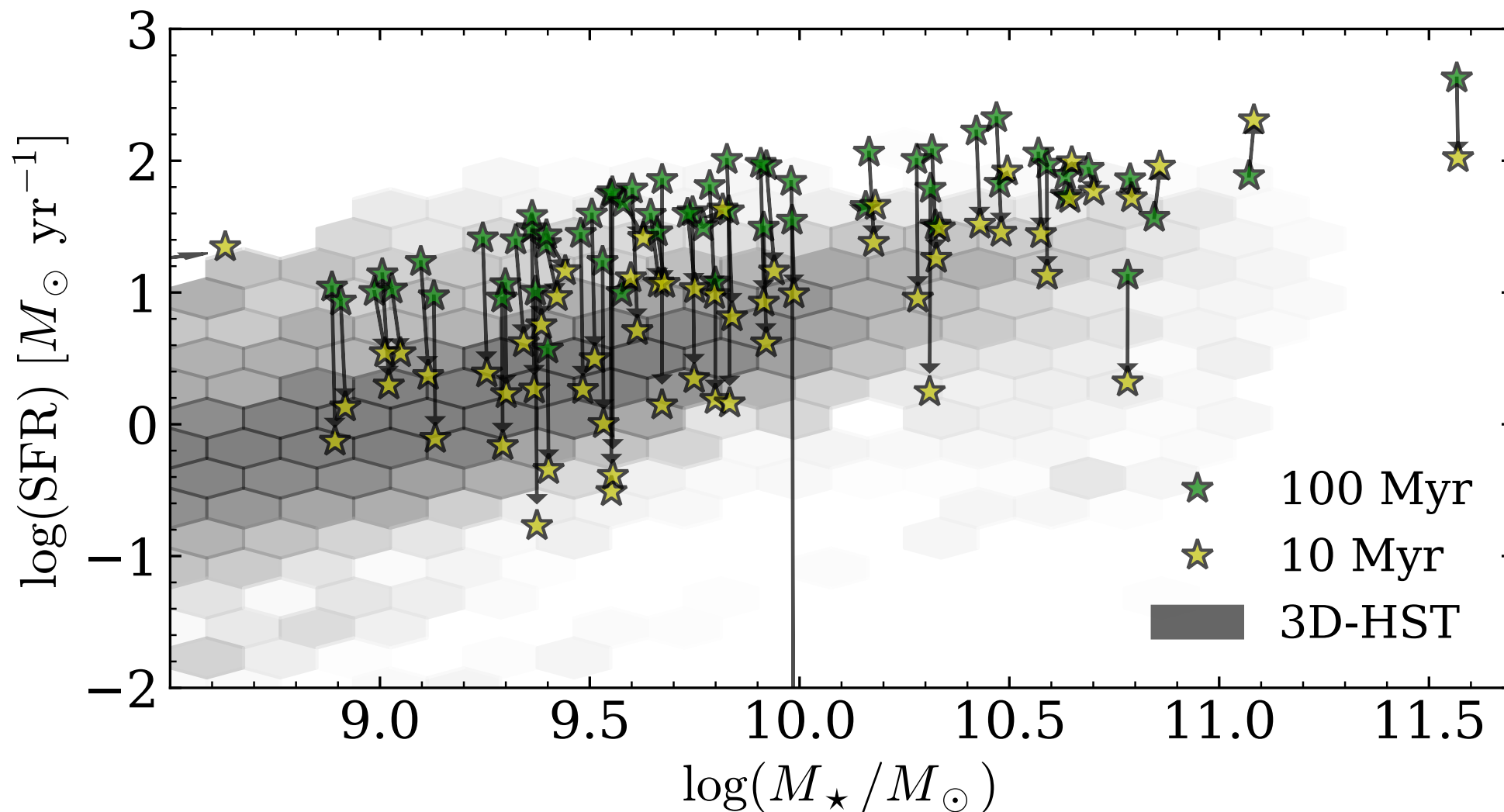
2 scenarios:

1. Compaction of gas into galactic center
2. Increase in clump accretion rate



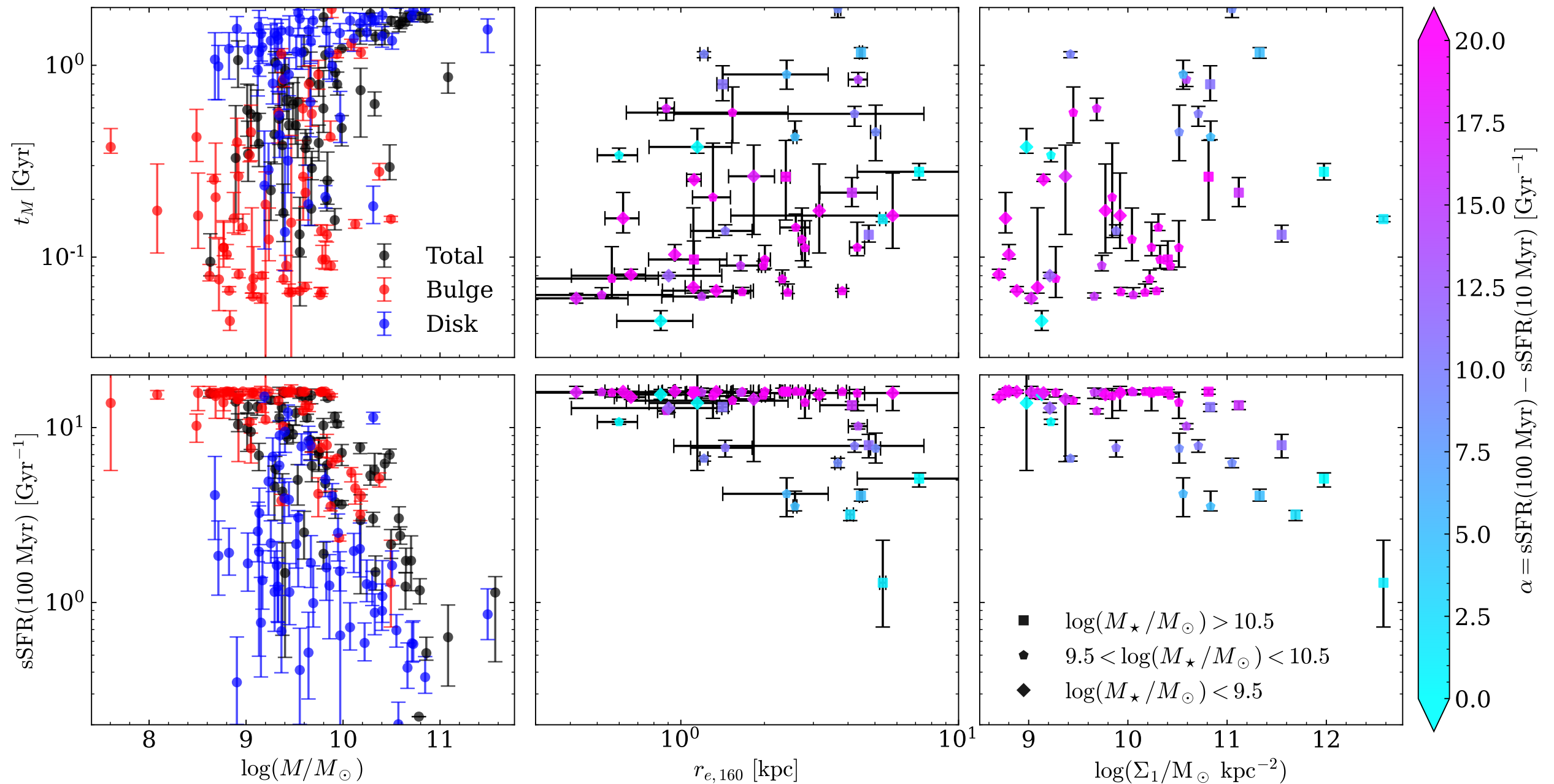
Main sequence evolution

Majority of galaxies experience a steep decrease in SFR, which seems to lessen with increasing mass

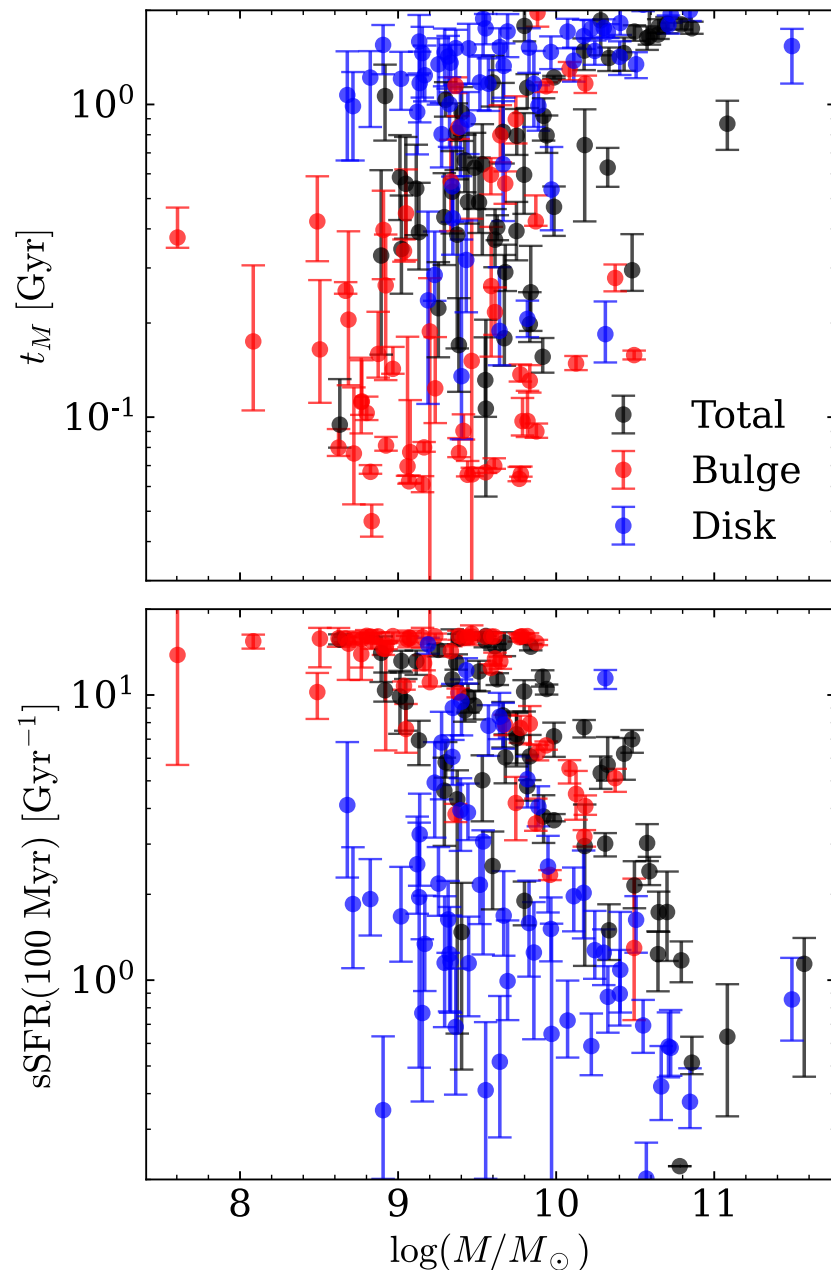


Ages and SFRs

Compare compactness with SFH parameters



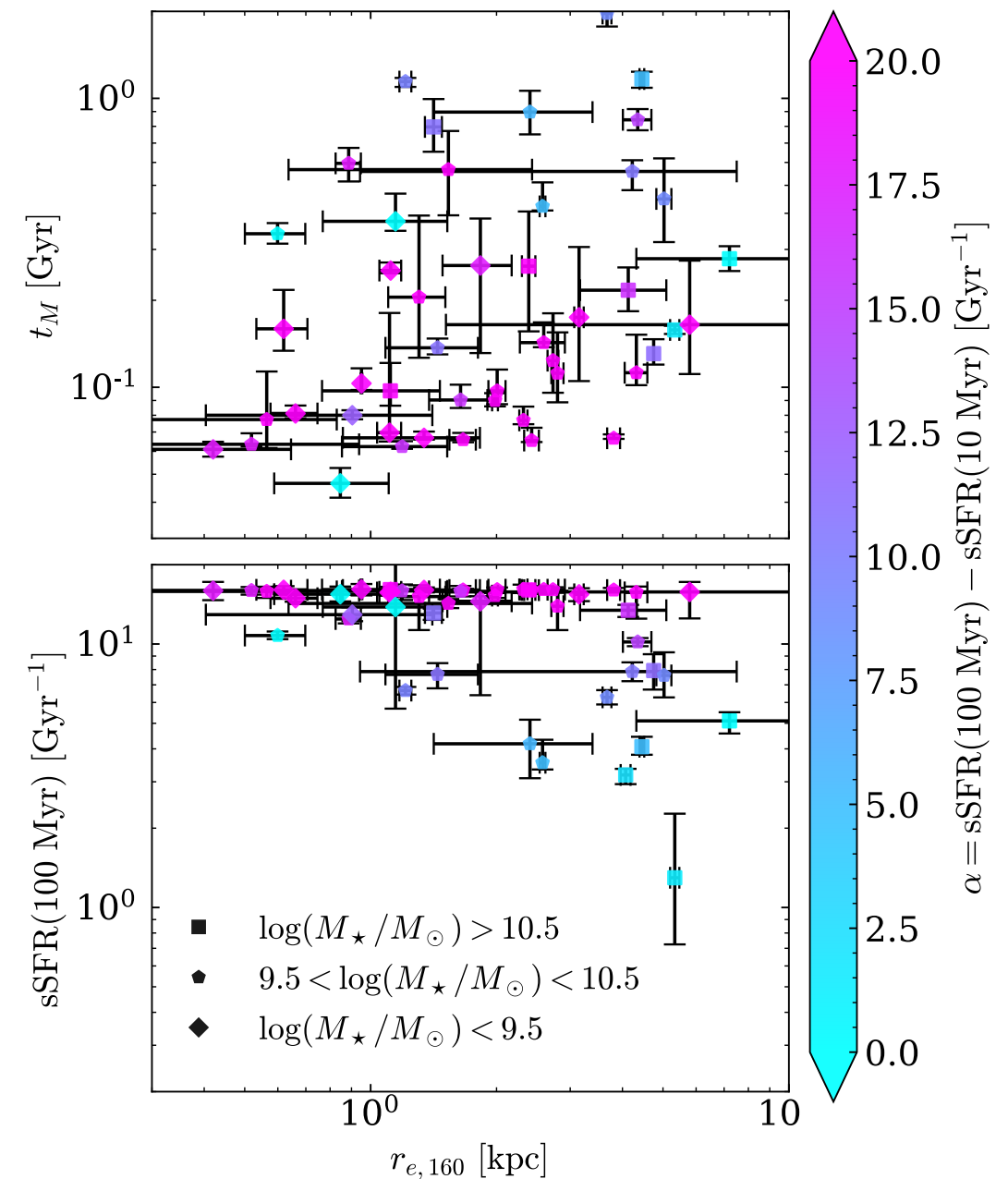
Ages and SFRs



- Bulges are younger and have higher sSFR than disks and the overall galaxy
- More massive bulges have lower sSFR and are older than lower mass bulges

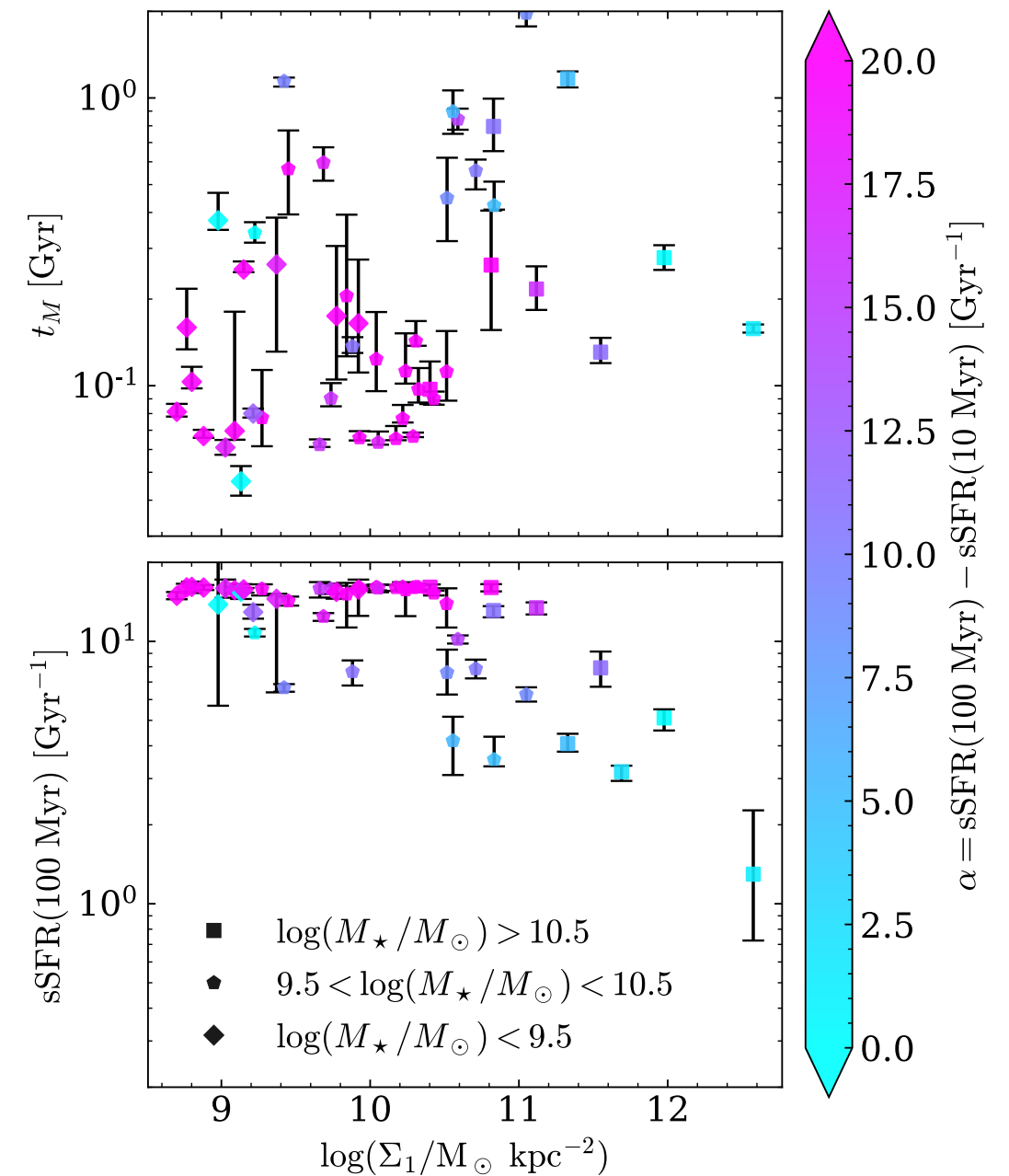
Ages and SFRs

- Younger galaxies have decreased more in sSFR
- Less massive ($\log M < 10.5$) galaxies have intense burst in star formation
- No trend in size



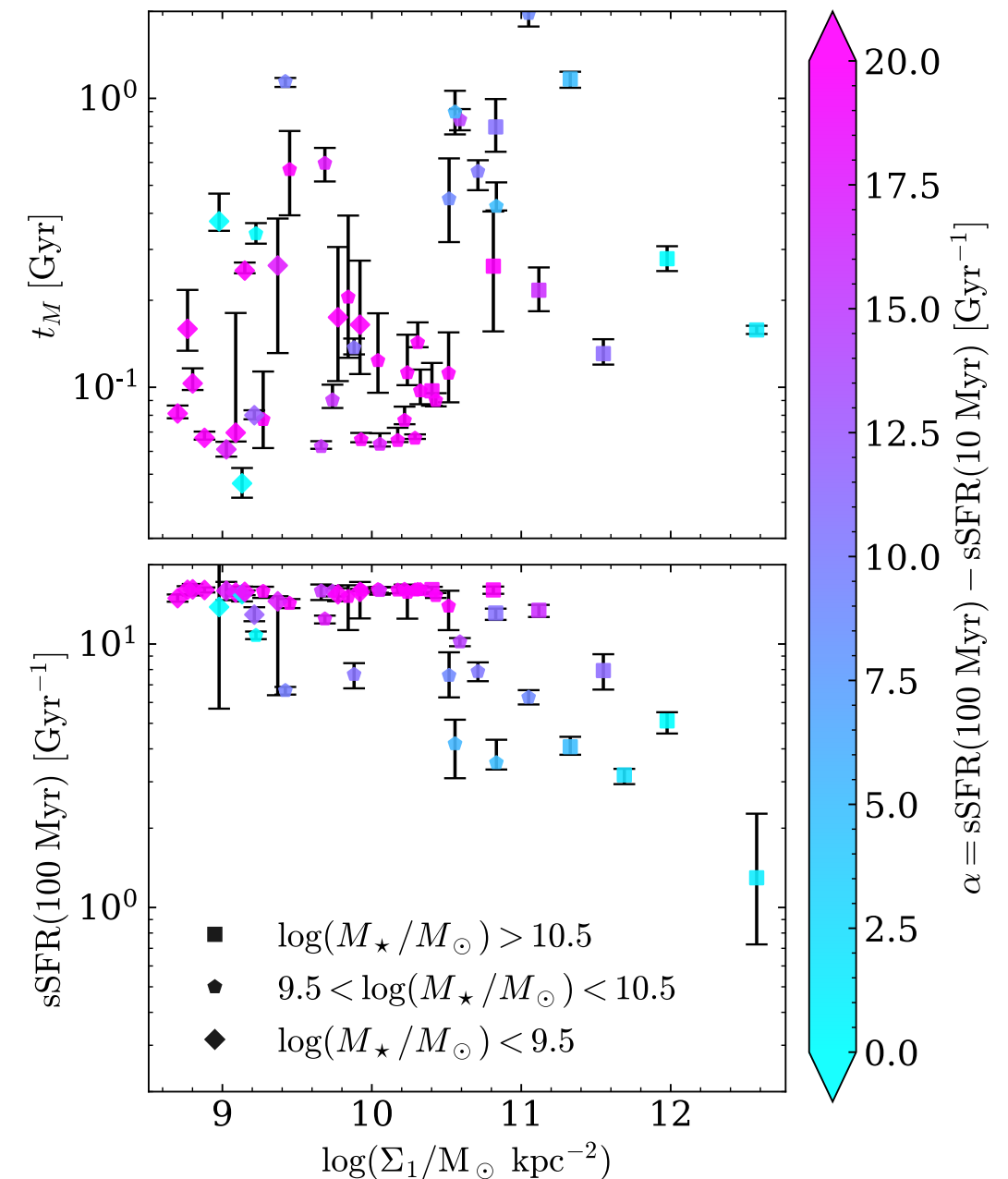
Ages and SFRs

- Younger galaxies have decreased more in sSFR
- Less massive ($\log M < 10.5$) galaxies have intense burst in star formation
- No trend in size or density



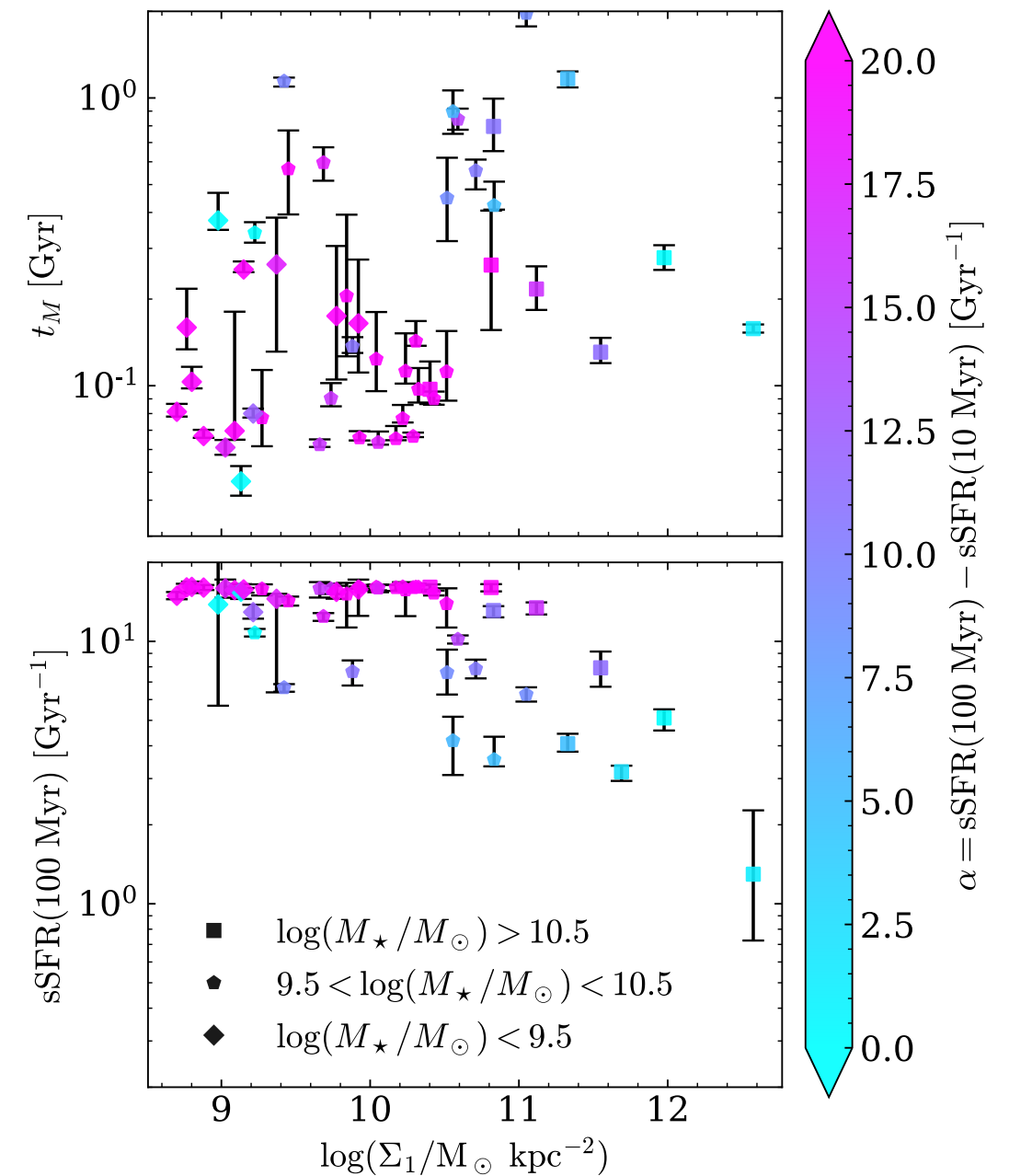
Ages and SFRs

- Younger galaxies have decreased more in sSFR
- Less massive ($\log M < 10.5$) galaxies have intense burst in star formation
- No trend in size or density
 - ▶ Compactness is not a factor in forming the bulge



Ages and SFRs

- Younger galaxies have decreased more in sSFR
- Less massive ($\log M < 10.5$) galaxies have intense burst in star formation
- No trend in size or density
 - ▶ Compactness is not a factor in forming the bulge
 - ▶ Clump accretion may be responsible



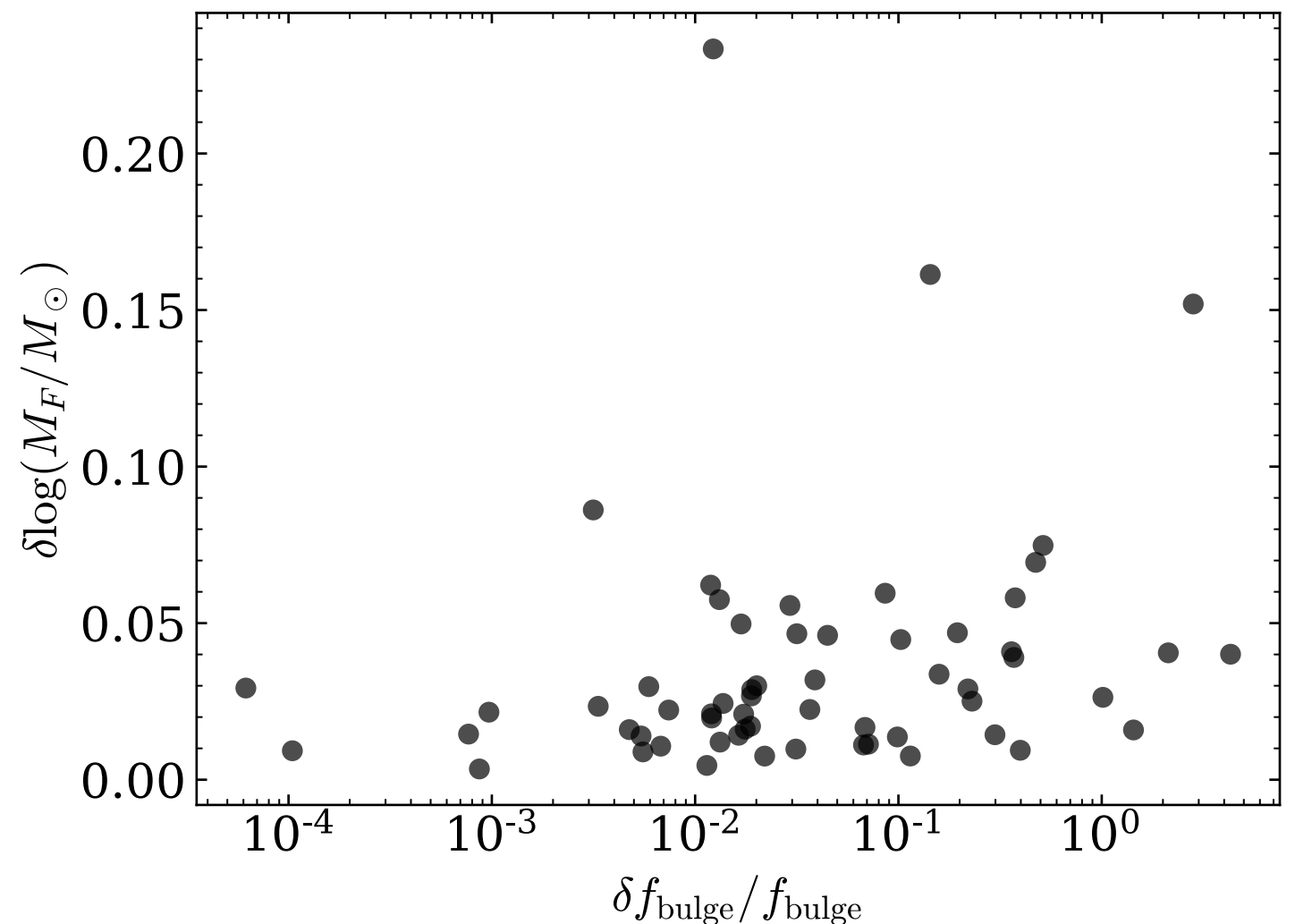
Uncertainties and future steps

- SED fitting and measuring nonparametric SFHs is uncertain
- Bulge decomposition and iterative photometry methods add to uncertainties
- Effect of different models/priors can be significant

Uncertainties and future steps: decomposition

Monte-Carlo sampling of bulge flux:

- Straightforward
- Computationally expensive



Uncertainties and future steps: metallicity priors

- For these results, assume disk dominates metallicity of galaxy
 - Know MW bulge is metal poor
- Disk doesn't always dominate light
- Future tests:
 1. Metallicity prior on bulge, not disk
 2. Metallicity prior on both
 3. Attempt to incorporate spectra for subcomponents
- In general, bulge and disk metallicities are comparable

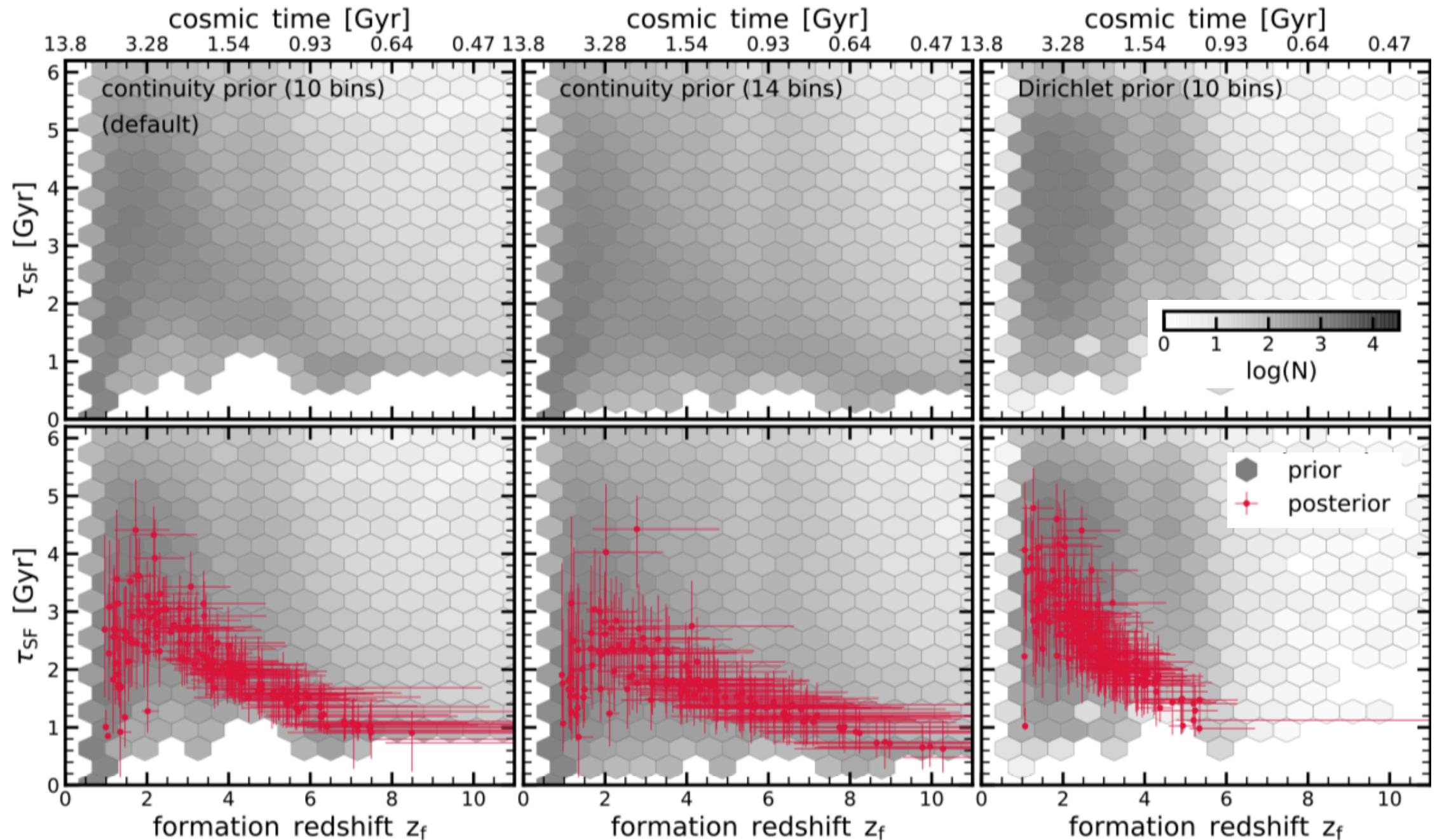
Uncertainties and future steps: SFH priors

- Dirichlet and continuity prior both model wide range of SFHs well
- Dirichlet prior may be better for burstier SFHs (tunable with α parameter)
- Confirming certain features still exist with a different SFH prior ensures these features are more likely to be real

Summary

- Prospector SED fits to decomposed central and outer components of 60 $z \sim 2.3$ main sequence, star-forming galaxies
- Iterative method to incorporate IRAC and ground-based K -band into decomposed SED fits
- SFHs indicate central regions formed in burst of star formation
- Burst of star formation lean towards increased clump accretion, not a compaction event
- Future steps will be crucial in verifying these results

Uncertainties and future steps: priors



Tacchella+21